NOVEL MECHANISMS GOVERNING SKELETAL MUSCLE MITOCHONDRIAL BIOENERGETICS: OXPHOS EFFICIENCY AND cAMP/PKA SIGNALING

by

Daniel Stephen Lark

June 2014

Director of Dissertation: P. Darrell Neufer

Department of Kinesiology

Understanding the regulation of cellular metabolism is paramount to treating the growing prevalence of metabolic disease worldwide. In cellular metabolism, mitochondrial oxidative phosphorylation (OXPHOS) plays a key role as it is a primary source of energy and the governor of cellular redox homeostasis. A fundamental aspect of mitochondrial function is that cellular metabolic demand requires a corresponding increase in flux through OXPHOS; however, the regulation of OXPHOS is incompletely understood. Herein, two hypotheses were tested: 1) OXPHOS efficiency increases as a function of metabolic demand to allow mitochondria to maximize ATP synthesis at a given level of O_2 flux and 2) that OXPHOS is regulated by cAMP/PKA signaling within skeletal muscle mitochondria. First, in permeabilized myofibers (PmFBs) from mouse skeletal muscle and myocardium, the data provided herein demonstrate that OXPHOS efficiency increases from ~20% to >70% from resting [ADP] to [ADP] found during exhaustive exercise in skeletal muscle, whereas [ADP] in the myocardium remains static (at ~75-100 μM) regardless of workload. Importantly, in the presence of small changes in [ADP] (e.g. 5-20 μM), ATP synthesis increased independent of an increase in JO_2, suggesting that skeletal muscle mitochondria can accommodate increased metabolic demand without a requisite increase in O_2 flux, suggesting a decrease in proton leak. Second, it was

demonstrated that tricarboxylic acid (TCA) cycle flux alone is insufficient to increase cAMP levels in isolated skeletal muscle mitochondria. However, pharmacological inhibition of PKA impairs a multitude of mitochondrial function outcomes in both liver and skeletal muscle that summarily implicate Complex I as a primary target. In conclusion, given the absolute necessity for coupled OXPHOS in the maintenance of energy homeostasis and the variety of diseases linked to decreased Complex I activity, the findings provided herein not only advance our current knowledge of mitochondrial bioenergetics, but provide a multitude of opportunities for future investigations.

NOVEL MECHANISMS GOVERNING SKELETAL MUSCLE MITOCHONDRIAL BIOENERGETICS: OXPHOS EFFICIENCY AND cAMP/PKA SIGNALING

A Dissertation

Presented to the Faculty of the Department of Kinesiology

East Carolina University

In Partial Fulfillment of the Requirements for the Degree

Doctor of Philosophy

By

Daniel Stephen Lark

June 13th, 2014

Novel Mechanisms Governing the Regulation of Mitochondrial Bioenergetics:

OXPHOS Efficiency and cAMP/PKA signaling

Novel Mechanisms Governing the Regulation of Mitochondrial Bioenergetics:

OXPHOS Efficiency and cAMP/PKA signaling

by

Daniel Stephen Lark

APPROVED BY:

DISSERTATION ADVISOR:_____

P. Darrell Neufer, Ph.D.

COMMITTEE MEMBER:_____

Ethan J. Anderson, Ph.D.

COMMITTEE MEMBER:_____

Carol A. Witczak, Ph.D.

COMMITTEE MEMBER:_____

David A. Brown, Ph.D.

CHAIR OF THE DEPARTMENT OF KINESIOLOGY

_____

Stacy R. Altman, J.D.

DEAN OF THE GRADUATE SCHOOL

_____

Paul J. Gemperline, Ph.D.

DEDICATION

This dissertation is dedicated to my wife and best friend Tara and our two little girls, Ava and Fiona.

ACKNOWLEDGEMENTS

My professional and intellectual growth, culminating in this report, would not have been possible without the guidance and support from a great number of people. From the day I arrived at ECU, I felt at home in Dr. Neufer's lab. As a master's student, learning from Drs. Ethan Anderson and Daniel Kane helped form the basis for my interest in, and understanding of, mitochondrial function. The depth of insight and ingenuity of Dr. Christopher Perry is only rivaled by his warm and gregarious personality, always willing to discuss any salient topic…over a potent potable. More recently, Drs. Laura Gilliam and Kelsey Fisher-Wellman have been role models by which I shaped my work ethic and approach to science. In addition, countless conversations with Cody Smith, Lauren Reese and Maria Torres have provided important insight and fresh perspectives for me in the last few years. Finally, Dr. Terence Ryan has been an excellent resource not only for data collection, but showing how the basic science we do in the lab translates to the clinic.

A number of faculty at ECU have influenced my intellectual development and have always been welcoming to me, particularly Drs.: David Brown, David Tulis, Michael Van Scott, Robert Caroll and Stefan Clemens in Physiology, Robert Hickner, Carol Witczak, Jeff Brault, Ron Cortright and Timothy Gavin in Kinesiology. I am also indebted to my fellow graduate students, in particular, Drs. Jill Maples, Joseph Pierce, Leslie Thompson and Fatiha Moukdar, as well as soon to be Dr. Lalage Katunga for their interactions over the course of my time here. Of course,

my work would not have been accomplished without the terrific administrative and technical staff both in the Neufer lab and in the Physiology and Kinesiology offices.

I have had the distinct honor of working with a number of investigators outside of my dissertation during my time here at ECU. I sincerely thank Drs. David Brown, Ethan Anderson, Deborah Muoio and Graham Holloway for the opportunity to broaden my scientific horizons through collaboration with their respective laboratories.

I owe an insurmountable amount of gratitude to my mentor, P. Darrell Neufer, for his guidance and support throughout my time here. Working under his tutelage has easily been the most empowering experience in my life. I am most grateful for his unique mentoring style which engenders independently thinking scientists, so called “mitochondriacs”.

My parents have supported me for my entire life, but never more so than while I was here at ECU. Their belief that I “could be anything I wanted to be” really drove me to pursue my passions in life that ultimately led me into a life of science.

During my time here, no one has been more influential on my success than Tara, my wife and best friend. She has made tremendous personal and professional sacrifices for me to pursue my degree here and for that, I will be forever indebted to her.

TABLE OF CONTENTS

ABSTRACT i

TITLE PAGE iii

COPYRIGHT PAGE iv

SIGNATURES PAGE v

DEDICATION vi

ACKNOWLEDGEMENTS vii

TABLE OF CONTENTS ix

LIST OF FIGURES xi

LIST OF SYMBOLS AND ABBREVIATIONS xiii

CHAPTER 1: REVIEW OF LITERATURE

Mitochondrial Bioenergetics in the Context of Redox Biology 1

Mitochondrial Proton Leak: Mechanisms and Relevance 4

Experimental Determination of OXPHOS 5

Mechanistic ATP/O ratios 7

Experimental ATP/O ratios 8

cAMP/PKA signaling 9

Mitochondrial cAMP/PKA Signaling 10

Conclusions 11

CENTRAL HYPOTHESIS 12

CHAPTER 2: DEMAND-DRIVEN ENHANCEMENT OF MITOCHONDRIAL OXIDATIVE PHOSPHORYLATION EFFICIENCY IN PERMEABILIZED MYOFIBERS

ABSTRACT 14

INTRODUCTION 15

EXPERIMENTAL PROCEDURES 16

RESULTS AND DISCUSSION 18

CHAPTER 3: PKA ACTIVITY GOVERNS OXIDATIVE PHOSPHORYLATION KINETICS AND OXIDANT EMITTING POTENTIAL AT COMPLEX I IN PERMEABILIZED MYOFIBERS

SUMMARY 41

HIGHLIGHTS 41

INTRODUCTION 42

METHODS 44

RESULTS 47

DISCUSSION 53

CHAPTER 4: INTEGRATED DISCUSSION 69

REFERENCES 78

APPENDIX A: ANIMAL USE PROTOCOL APPROVAL 93

LIST OF FIGURES

FIGURE 1: Assay chemistry, instrumentation and validation. 26

FIGURE 2: A representative experiment performed to determine OXPHOS efficiency kinetics. 28

FIGURE 3: Rates of ATP synthesis and O2 consumption measured as a function of metabolic demand in PmFBs. 30

FIGURE 4: OXPHOS Efficiency as a function of metabolic demand in PmFBs. 32

FIGURE 5: Adenylate kinase is a source of ATP production in PmFBs 34

FIGURE 6: Effects of AK inhibition of ATP/O ratio in PmFBs. 36

FIGURE 7: A working hypothesis for demand-driven enhancement of OXPHOS efficiency. 38

FIGURE 8: TCA-cycle dependent cAMP levels and effect of exogenous cAMP on respiratory capacity in isolated mitochondria. 59

Supplemental Figure, related to Figure 8. 61

FIGURE 9: Pharmacological inhibition of PKA dose-dependently decreases Complex I- but not Complex II-supported respiration in isolated liver mitochondria. 63

FIGURE 10: Effects of PKA inhibition on substrate oxidation kinetics and oxidant production in PmFBs. 65

FIGURE 11: Effects of PKA inhibition on ADP kinetics and OXPHOS efficiency in PmFBs. 67

LIST OF SYMBOLS AND ABBREVIATIONS

2-HE	2-Hydroxyestradiol
2-ME	2-Methoxyestradiol
ADP	Adenosine Diphosphate
ANT	Adenine Nucleotide Translocase
AKAP	A Kinase-Associated Protein
Ap5A	P1,P5-Di(adenosine-5′) pentaphosphate
ATP	Adenosine Triphosphate
ATP/O	Ratio of ATP produced to oxygen consumed
AZA	Acetazolamide
BSA	Bovine Serum Albumin
CaMK	Calcium/Calmodulin-activated Protein Kinase
cAMP	Cyclic adenosine monophosphate
COX	Cytochrome Oxidase
Cr	Creatine
Δp	Protonmotive Force
ETS	Mitochondrial Electron Transfer System
FCCP	Trifluoromethoxy carbonylcyanide phenylhydrazone
G6P	Glucose-6-Phosphate
G6PDH	Glucose-6-Phosphate Dehydrogenase
GPx	Glutathione Peroxidase
GR	Glutathione Reductase
GSH	Reduced Glutathione
GSSG	Oxidized Glutathione
H_2O_2	Hydrogen Peroxide

H89	5-Isoquinolinesulfonamide
HK	Hexokinase
IC_{50}	Half maximal inhibitory concentration
*J*ATP	Rate of mitochondrial ATP production
JO_2	Rate of Mitochondrial Oxygen Consumption
KH7	2-(1H-benzimidazol-2-ylthio)-2-[(5-bromo-2-hydroxyphenyl)methylene]hydrazide, propanoic acid
LV	Left Ventricle of the heart
mOEP	Mitochondrial Oxidant Emitting Potential
mOPP	Mitochondrial Oxidant Producing Potential
NAD^+	Oxidized Nicotinamide Dinucleotide
NADH	Reduced Nicotinamide Dinucleotide
$NADP^+$	Oxidized Nicotinamide Dinucleotide Phosphate
NADPH	Reduced Nicotinamide Dinucleotide Phosphate
NNT	Nicotinamide Dinucleotide Transhydrogenase
OXPHOS	Oxidative Phosphorylation
PDE	Phosphodiesterase
PDHC	Pyruvate Dehydrogenase Complex
RG	Red portion of gastrocnemius muscle
PCr	Phosphocreatine
P_i	Inorganic Phosphate
PKA	Protein Kinase A
PmFB	Permeabilized Myofiber Bundle
RCR	Respiratory Control Ratio
ROCK	Rho-associated Protein Kinase
ROS	Reactive Oxygen Species

Rot	Rotenone
sAC	Soluble form of adenylyl cyclase
SUIT	Substrate-uncoupler-inhibitor-tiration
TCA	Tricarboxylic Acid Cycle
TmAC	Transmembrane form of adenylyl cyclase
TrxR	Thioredoxin Reductase
UCP	Uncoupling Protein
WG	White portion of gastrocnemius muscle

CHAPTER 1: REVIEW OF LITERATURE

Mitochondrial Bioenergetics in the Context of Redox Biology

The ability of the mitochondrion to generate adenosine triphosphate (ATP) is dependent on mitochondrial electron transfer because the concomitant extrusion of protons from the mitochondrial matrix creates an electrochemical gradient (more H^+ outside than inside), which establishes/maintains a proton motive force (Δp). The potential energy stored as Δp is then used by ATP synthase to generate ATP. ATP is then exchanged across the inner membrane with adenosine diphosphate (ADP) + inorganic phosphate (P_i) via adenine nucleotide translocase (ANT). The coupling of substrate oxidation that results in establishing Δp and the production of ATP is summarily referred to as oxidative phosphorylation (OXPHOS).

OXPHOS is essential for eukaryotic energy homeostasis and can be wholly described within the context of redox biology. Redox biology is the study of oxidation/reduction reactions that impact innumerable aspects of cellular function and homeostasis, including mitochondrial electron transfer [1]. Redox biology is fundamental to mitochondrial electron transfer because it explains how the “circuitry”, via maintenance of redox couples, determines the redox potentials throughout the cell, and therefore the ability of electrons to move through the mitochondrial electron transfer system (ETS). Redox couples are discreet molecules that exist in either reduced (RH) or oxidized (R^+) forms. For example, nicotinamide dinucleotide (NADH) serves as the substrate for Complex I of the ETS; however, the driving force for oxidation of NADH is determined by the NADH/NAD^+ ratio, not [NADH] alone [2]. Conversely, the driving force for NADH-producing reactions, like that

catalyzed by the pyruvate dehydrogenase complex (PDHC), is also largely determined by the $NADH/NAD^+$ couple [3]. In this albeit over simplified system, a high $NADH/NAD^+$ ratio translates to oxidation of NADH being favorable; conversely, a low $NADH/NAD^+$ ratio translates to a propensity for NAD^+ reduction. In the context of redox biology, the effect of $NADH/NAD^+$ ratio on a given biochemical system is complicated by concomitant reactions. For example, in the case of mitochondrial electron transfer, NADH oxidation by Complex I results in electron flow through iron/sulfur complexes and ultimately terminates by reducing ubiquinone. Electron flow through Complex I and proton efflux from the matrix are mutually inclusive events, with proton efflux occurring against its electrochemical gradient, ultimately to establish and maintain Δp, the potential energy used to drive ATP synthesis. Thus, if Δp is high, proton efflux is less favorable, so the rate of NADH oxidation by Complex I will decrease, reflecting an inability to pump protons. In this way, Δp marries OXPHOS and redox biology and therein, illustrates one of many roles that redox biology plays in the context of mitochondrial bioenergetics.

Another excellent example of the interplay between mitochondrial bioenergetics and redox biology is found when considering the maintenance of the cellular redox environment. An analog to the cellular redox environment is our planet: it is made up of a collection of ecosystems that independently maintain homeostasis but are under the control of a central regulator (e.g. the sun). Similarly, intracellular "ecosystems" are separated by membranes [4], each one existing in its ideal redox homeostatic environment and, in most cases, under the central control of the mitochondrion. This is achieved in part because the mitochondrial matrix is more reduced than the surrounding redox environment (e.g. cytosol) and the ETS is a primary source of hydrogen peroxide (H_2O_2), the oxidative "input" to the redox circuitry [1, 5]. H_2O_2 generated by the ETS is constant, occurring at low levels under normal resting conditions (13, 69), such that redox couples throughout the proteome are maintained in a mostly, but never completely, reduced state [5]. When mitochondrial H_2O_2 is increased, which occurs under a

number of physiological conditions, some of which are pathological (e.g. high fat feeding and obesity [6, 7], ischemia [8] and inflammation [9]), redox couples become progressively more oxidized. As the matrix redox environment becomes more oxidized, H_2O_2 production exceeds scavenging and oxidants escape the matrix and reach other compartments. This "emission" of H_2O_2 can shift the redox environment of these other compartments, leading to modifications in protein function that are commonly associated with "oxidative stress". However, these modifications are largely reversible, and the mitochondrion possesses a high capacity to buffer H_2O_2. This is possible in large part because in addition to serving as substrate for OXPHOS, NADH is also substrate for nicotinamide nucleotide transhydrogenase (NNT), which oxidizes NADH to reduce $NADP^+$ while consuming Δp [10], thus increasing the NADPH/$NADP^+$ ratio. NADPH is the substrate for glutathione reductase (GR), which reduces oxidized glutathione (GSSG), forming two glutathione (GSH). GSH is a key redox buffering component as it can scavenge H_2O_2 directly via glutathione peroxidase (GPx) or indirectly by reducing thioredoxin via thioredoxin reductase (TrxR). In addition to NADPH production via NNT to buffer oxidants, dissipation of Δp profoundly decreases H_2O_2 production from the ETS [11]. The balance between oxidant production and scavenging within the mitochondrial matrix is a major determinant of the overall regulation of the cellular redox environment as increased mitochondrial oxidant production is capable of shifting the GSH/GSSG ratio of the entire cell [6].

In addition to acting as an oxidant scavenger, GSH can also impart post-translational modification to proteins, known as glutathionylation [12-14]. Glutathionylation of mitochondrial proteins in skeletal muscle and myocardium occurs largely through glutaredoxin 2 (Gr2) [15-17] in a similar fashion to other post-translational modifications (e.g. phosphorylation) where it can modulate the activity, structure and/or function of proteins throughout the proteome. The functions of GSH are ultimately under the control of redox circuitry, as a change in the NADH/NAD^+ ratio will correspondingly alter the NADPH/$NADP^+$ ratio. A change in the

NADPH/$NADP^+$ ratio will alter the redox potential of a given GSH-dependent reaction, which would determine the likelihood of a protein to be glutathionylated, or whether a given cysteine in a particular cellular compartment is oxidized or reduced [18]. Altogether, mitochondrial oxidation production and emission oxidizes the redox environment (e.g. ↓GSH/GSSG), depressing redox circuitry (e.g. ↓NADH/NAD^+) and leading to alterations in cellular physiology (e.g. increased substrate oxidation to replenish NADH). In this way, redox biology describes how the cell and, in particular the mitochondria, maintain a collection of circuits comprised of molecules maintaining redox potentials that integrate cellular energetics (e.g. NADH/NAD^+) and metabolism.

Mitochondrial Proton Leak: Mechanisms and Relevance

Proton leak is an integral aspect of non-shivering thermogenesis in mammals as it ultimately accounts for between 20-50% of basal energy expenditure in mammals [19]. Sources of mitochondrial proton leak and their regulation have been extensively reviewed [20, 21] with two endogenous sources of mitochondrial proton leak being of central importance: uncoupling proteins (UCPs) and adenine nucleotide translocase (ANT).

UCPs are a family of proteins located in the mitochondrial inner membrane that share sequence homology but whose expression is largely isoform-dependent [22]. For example, UCP1 is found exclusively in brown adipose tissue [23] with its activity and expression levels extensively described [22]. Conversely, despite considerable (>50%) sequence homology with UCP1, the physiological roles of UCP2 and UCP3 are far less understood. UCP2 is ubiquitously expressed [24-26] and of particular note, has been shown to be an important regulator of insulin secretion and neuronal plasticity [24, 25]. UCP3 is predominantly expressed in skeletal muscle and a growing body of evidence has demonstrated that the physiological function of UCP3 is as a mitochondrial fatty acid transporter [27-30] that is capable of decreasing mitochondrial H_2O_2

production [29, 31, 32]. UCP3 overexpressing mice are protected from diet-induced obesity and insulin resistance [33], while a number of studies have provided evidence either for [30] [34] [35, 36] or against [29, 37-39] UCP3 as a source of mitochondrial proton leak. Altogether, while the existing evidence does not conclusively demonstrate a role for UCP3 in proton conductance, it does appear to alter mitochondrial bioenergetics indirectly either by decreasing mitochondrial H_2O_2 production or changing intramitochondrial fatty acid content/composition.

ANT is an essential mitochondrial inner membrane protein that is responsible for exchanging ADP and ATP across the mitochondrial inner membrane. Importantly, ANT-mediated influx of ADP from the intermembrane space consumes Δp as it occurs in synchrony with $P_i + H^+$. ANT not only consumes Δp as a result of nucleotide exchange, since previous work by Brand et al. [40] has elegantly shown that ANT protein content is a primary determinant of basal proton conductance. ANT activity is inhibited by lipid peroxidation products (e.g. 2- and 4-hydroxynonenal) [41], but enhanced by AMP [42] and fatty acids [43]. Altogether, ANT represents an alternative source of proton leak to that mediated by UCPs and may be an essential source of proton conductance both at rest and during metabolic demand in skeletal muscle mitochondria.

Experimental Determination of OXPHOS

Experimental measurement of OXPHOS necessitates an understanding of the terminology used to define states of mitochondrial O_2 consumption. The conventions for defining respiratory states were originally established by Chance and Williams in the 1950's [44] and reflected the step-wise procedure of measuring respiration with their established method. State 1 respiration refers to the rate of O_2 consumption (JO_2) that occurs in the presence of mitochondria only, prior to the addition of respiratory substrates (e.g. glutamate or succinate), ADP or inhibitors. This state is thought to be essentially artifactual O_2 consumption from the materials inherent to the

measurement system. For example, Teflon and other plastics used in the jacketing, stopper or stir bar can release or absorb O_2 from liquids [45], thus air calibration of media and subtraction of background JO_2 are essential steps needed for accurate determination of mitochondrial function [46, 47]. State 2 respiration is that which occurs in the presence of ADP but prior to the addition of respiratory substrates, resulting in a low rate of O_2 consumption that is limited by substrate availability. State 3 respiration is described as the rate of O_2 consumption in the presence of both substrate and ADP, when OXPHOS to actively generating ATP. Eventually, ADP is exhausted and respiration returns to essentially basal conditions, defined as state 4.

Notably, more recent conventions have been described by Nicholls and Ferguson in their seminal text, *Bioenergetics 4* [48] that better reflect the steps taken to assess mitochondrial function using more technically advanced substrate-uncoupler-inhibitor-titration (SUIT) protocols. For example, according to Nicholls and Ferguson, state 2 is defined as the rate of O_2 consumption in the presence of respiratory substrates instead of ADP. In this case, state 2 respiration is empirically equivalent to state 4 described by Chance and Williams in that the rate of respiration is directly proportional to the rate of proton leak back into the matrix. State 4, although theoretically equivalent between conventions, using SUIT protocols is often achieved following the addition of an inhibitor of ATP synthase (e.g. oligomycin). Regardless of semantic differences between conventions, standard practice in the literature is to report state 4 respiration as JO_2 in the presence of substrates but in the absence of ATP synthesis, either prior to addition of ADP or following addition of a respiratory inhibitor [46, 47, 49].

A common strategy when studying mitochondrial bioenergetics is to determine the maximal capacity of O_2 consumption in the presence of saturating amounts of respiratory substrates and ADP. While this approach provides some information on how mitochondria are acting in a given tissue or in response to a treatment or genetic manipulation, the use of steady-state kinetic analyses can provide mechanistic insight where measuring maximal capacity cannot. To

measure steady-state kinetics, substrates or ADP are titrated during a protocol from very low to very high concentrations. For example, by titrating ADP, an investigator can determine how "sensitive" OXPHOS, as an entire system, is to metabolic demand by applying Michaelis-Menten like kinetic analyses to the data, yielding two variables: the concentration of substrate (e.g. ADP) required to elicit ½ maximal JO_2, defined as K_m and 2) the predicted maximal JO_2, defined as V_{max}. The physiological relevance of this assessment in a metabolically dynamic tissue like skeletal muscle is readily apparent since [ADP] can increase > 4 fold during exhaustive exercise in human skeletal muscle [50]. By measuring only maximal respiratory capacity, interpretations of the effects of an intervention (e.g. exercise training) on OXPHOS may not be fully realized. Similarly, titration of respiratory substrates (e.g. pyruvate or succinate) can be used to ascertain the sensitivity of OXPHOS to a particular substrate or combination of substrates. This approach can be used to understand the interplay between the ETS and mitochondrial dehydrogenases responsible for oxidizing substrates. Ultimately, the opportunities provided by kinetic analysis of OXPHOS yield considerably more insight than the more simplistic assessment of maximal respiratory capacity, although both approaches have their merits.

Mechanistic ATP/O ratios

Determining the mechanistic, or theoretically "maximal", level of OXPHOS efficiency requires deconstruction of its two requisite components: 1) electron flow that facilitates proton efflux from the matrix and 2) proton influx back into the matrix, resulting in either synthesis of ATP or thermogenic proton leak. Since mitochondrial electron flow and H^+ being pumped out of the matrix are inexorably linked, the amount of H^+ pumped per oxygen atom consumed can be divided by the amount of H^+ needed to synthesize ATP to define OXPHOS efficiency as the ATP/O ratio [45]. Previous studies have elucidated stoichiometric values for each aspect needed, so a predicted value of OXPHOS efficiency can be established based on the

cumulative reactions that begin with NADH oxidation and terminate at ATP synthesis and O_2 consumption. Currently accepted literature values state that 4 H^+ are pumped from Complex I [51], 2 H^+ are pumped from Complex III [52] and 4 H^+ from Complex IV [53] per NADH oxidized. This yields a total of 10 H^+ being extruded from the mitochondrial matrix per NADH oxidized (or pair of electrons transported). The F_O-F_1 ATP synthase is a fascinating enzyme in that it has a molecular motor consisting of c-subunits that generate ATP by using the energy released as H^+ re-enters the matrix down its concentration gradient. With each 360° rotation of this motor, it is thought that three ATP molecules are produced [54]. Defining the molecular mechanism(s) by which ATP synthase operated was fundamental to our understanding of bioenergetics, but it was not until the crystal structure of ATP synthase was revealed by Stock et al. in 1999 [54] that the stoichiometry of H^+/ATP could begin to be realized. These investigators found that yeast ATP synthase possessed 10 c-subunits, meaning that a full rotation of ATP synthase would require 10/3 = 3.33 H^+/ATP. While this discovery profoundly changed our view of bioenergetics, it was not until more recently that the c-subunit stoichiometry of mammalian ATP synthase was provided by Watt et al. in 2010 [55]. These investigators revealed that bovine heart mitochondrial F_O-F_1 ATP synthase possessed 8 c-subunits, suggesting that only 2.7 H^+ were required to synthesize ATP. Subsequent to ATP synthesis, ANT exchanges ATP for ADP + P_i across the mitochondrial inner membrane. Although H^+ is not used in this process, there is a net positive charge associated with this exchange and thus an additional H+ is added to the H+/ATP stoichiometry, summarily equaling 3.7 H^+/ATP. Using these values, the maximal ATP/O ratio when exclusively oxidizing NADH would be 10/3.7 = 2.7 ATP molecules per O (not O_2) consumed.

Experimental ATP/O ratios

Measuring OXPHOS efficiency experimentally has been performed a number of different ways, and as might be expected, values vary greatly throughout the literature. As far back as 1940's,

ATP/O ratios have been reported in mitochondrial preparations [56]. The most common method to experimentally determine OXPHOS efficiency has been by measuring the amount of O_2 consumed in response to a given amount of ADP added to a mitochondrial sample, originally demonstrated by Chance and Williams [44]. This approach, which is still widely used today, yields the semantically distinct ADP/O ratio. However, a more direct approach to determining OXPHOS efficiency has recently been described by Gouspillou et al. [57] where both ATP synthesis and O_2 consumption are directly measured simultaneously and in real time. Perhaps most interestingly, this method allowed for the determination of ATP/O at different concentrations of ADP, thus providing an index of OXPHOS efficiency as a function of metabolic demand. These same authors have provided evidence that OXPHOS efficiency is altered by aging [58], providing some initial evidence that OXPHOS efficiency may degrade, as many other aspects of physiology do, with age.

cAMP/PKA signaling

Post-translational modifications to proteins can occur in a variety of ways, but historically, the most heavily studied has been phosphorylation. Phosphorylation of proteins is catalyzed by kinases, a class of proteins that transfer the γ-phosphate group of ATP to a serine, tyrosine or threonine residue of a target protein(s). One ubiquitously expressed protein kinase in eukaryotic cells is protein kinase A (PKA), a tetrameric serine/threonine kinase consisting of two catalytic (C) domains and two regulatory (R) domains. PKA is activated by the classic 2nd messenger molecule cyclic AMP (cAMP), first described by Nobel laureate Earl Sutherland in 1958 [59].

The cAMP/PKA axis relies on adenylyl cyclases that can be either transmembrane-bound (TmAC) or soluble (sAC), the latter being first described in 1999 [60]. The cAMP/PKA axis has been perhaps most heavily studied in the field of endocrinology, where a hormone (e.g.

glucagon) binds to an extracellular receptor, triggering a G protein-dependent cascade that activates TmAC inside the cell, resulting in an increase in intracellular cAMP production. cAMP then binds to the regulatory subunit of PKA, opening the ATP binding pocket in the C subunit, allowing for phosphorylation of target proteins. By contrast, sAC activity is regulated by calcium [61-63], bicarbonate [64] and ATP [61]. In this way, sAC is thought to be a physiological pH sensor [64] that is responsive to changes in oxidative metabolism. Intracellular cAMP levels are tightly regulated by synchronicity between ACs and phosphodiesterases (PDEs), a family of enzymes with four isoforms (PDEs 4, 7 and 8) that are specific for cAMP and five (PDEs 1-3, 10 and 11) that catabolize both cAMP and cGMP. PDE isoforms have distinct tissue and subcellular expression patterns that coincide with discreet compartmentalized cAMP-dependent signaling domains [62, 65-67].

Mitochondrial cAMP/PKA Signaling

There are a vast number of PKA targets that regulate a variety of cellular functions, a few of which are: glycogen metabolism, mitochondrial biogenesis and glucagon signaling. Substrates for PKA-dependent phosphorylation are not only numerous, but also encompass proteins found in a number of different subcellular domains, together suggesting that PKA is likely present in these different areas of the cell, including mitochondria in particular. Indeed, a number of independent reports have found PKA in mitochondrial fractions from a variety of different tissues [68-70]. Furthermore, recent work using a fluorescent PKA sensor targeted to mitochondria suggests that ~80% of mitochondrial PKA activity is within the matrix [71]. The subcellular localization of PKA is determined by a class of scaffolding proteins called A kinase anchoring proteins (AKAPs) [72-74]. Along with a number of other AKAPs, D-AKAP2, a dual role AKAP that binds to both the RI and RII regulatory subunits of PKA, is highly enriched in mitochondria of mouse, rat and human tissues [75]. Consistent with a mitochondrial cAMP/PKA cascade, sAC has been found in mitochondria [67], along with a PDE isoform (PDE2A)[66]. Illustrating

the relevance of a mitochondrial cAMP/PKA signaling pathway, a recent report has revealed that over 75 different mitochondrial proteins have consensus sites for PKA-dependent phosphorylation [76].

With overwhelming evidence that a cAMP/PKA signaling cascade is wholly located within the mitochondrial matrix, recent reports have begun to elucidate its possible regulatory function on OXPHOS. From these recent reports, two components of the ETS have been identified as likely targets of mitochondrial cAMP/PKA signaling in the context of OXPHOS: the 18kDa subunit of Complex I and cytochrome c oxidase (COX) of Complex IV. Sergio Papa and his colleagues have provided evidence over a nearly 20 year span that PKA-dependent phosphorylation of Complex I of the ETS regulates its assembly and activity [68, 77-81], findings that have been supported by independent groups [82, 83]. The link between PKA-dependent phosphorylation and Complex I deserves further exploration, particularly in light of recent findings suggesting that PKA-dependent phosphorylation of Complex I contributes to the pathoetiology of Down's syndrome [82]. In addition to Complex I, COX has been identified as a target of the mitochondrial cAMP/PKA axis [67, 84, 85]. COX is the terminal electron transferring enzyme of the ETS by catalyzing the hydration of molecular oxygen to form water, so its regulation by PKA likely has implications for the overall regulation of OXPHOS. Finally, identification of these phosphorylation sites has been accompanied by reports demonstrating the functional impact of mitochondrial cAMP/PKA signaling on OXPHOS [62, 67].

Conclusions

With the growing interest in the regulation of mitochondrial bioenergetics, understanding how OXPHOS is governed both by metabolic demand and via phosphorylation is central to identifying new treatments for mitochondrial diseases. With this goal in mind, the first project describer here was designed to test the hypothesis that OXPHOS efficiency increases as a

function of metabolic demand to maximize the ability of mitochondria to support energy homeostasis. Then, given the role of Complex I as both a source of H_2O_2 and a regulator of electron flow through the ETS, the second project in this report was designed to test the hypothesis that phosphorylation of Complex I determines the capacity and kinetics of mitochondrial substrate oxidation, ATP synthesis and oxidant production.

CENTRAL HYPOTHESIS

The goal of this dissertation was to determine whether mitochondrial OXPHOS efficiency increases as a function of metabolic demand and whether OXPHOS is regulated by PKA-dependent phosphorylation of ETS proteins. The overriding hypothesis was that enhanced OXPHOS efficiency is a requisite adaptation to metabolic demand and that PKA-dependent phosphorylation governs OXPHOS by regulating electron flow through Complex I.

In Chapter 2, a novel approach was developed, validated and then utilized to reveal demand-driven enhancement of OXPHOS efficiency as a common response in skeletal muscle and myocardial PmFBs. In Chapter 3, mitochondrial cAMP/PKA signaling was characterized in skeletal muscle, then using a comprehensive approach, pharmacological inhibition of PKA was demonstrated to preferentially inhibit electron flow via Complex I of the ETS but without altering OXPHOS efficiency. Altogether, it is concluded that demand-driven enhancement of OXPHOS efficiency is a common feature of mitochondria from striated muscle, and perhaps of all mitochondria, and is therefore a central feature of cellular metabolism, but the mechanism(s) regulating OXPHOS efficiency remain to be defined.

CHAPTER 2: DEMAND-DRIVEN ENHANCEMENT OF MITOCHONDRIAL OXIDATIVE PHOSPHORYLATION EFFICIENCY IN PERMEABILIZED MYOFIBERS

Daniel S. Lark[2,4], Terence E. Ryan[1,4], Ethan J. Anderson[3,4] and P. Darrell Neufer[1,2,4†]

Departments of [1]Physiology, [2]Kinesiology, [3]Pharmacology and Toxicology and [4]East Carolina Diabetes and Obesity Institute, East Carolina University, Greenville, North Carolina

Running Head: ATP/O in permeabilized mouse and human myofibers

† To whom correspondence should be addressed:

P. Darrell Neufer (NEUFERP@ECU.EDU) Department of Physiology, East Carolina University, East Carolina Heart Institute, Room 4101, 115 Heart Dr., Greenville NC 27834

ABSTRACT

The efficiency of oxidative phosphorylation (OXPHOS), quantified as the amount of ATP produced per oxygen atom consumed (ATP/O), is vital to maintaining proper myocyte energetics. However, despite its central importance, it is difficult to experimentally determine ATP/O ratio as a function of metabolic demand, and therefore, the relationship between OXPHOS efficiency and metabolic demand is poorly understood. In this report, we describe and validate a novel approach to simultaneously quantify ATP synthesis and O_2 consumption, thereby yielding ATP/O ratio, in permeabilized mouse myocardium and both oxidative and glycolytic skeletal muscle across a physiologically relevant range of [ADP]. With this technique, it was observed that ATP/O ratio increased as a function of [ADP] and may occur independent of an increase in O_2 consumption at low (5-20 μM) [ADP]. Pharmacological inhibition of adenylate kinase decreased *J*ATP in a tissue-specific fashion but did not alter ADP-dependent increases in OXPHOS efficiency. Summarily, these observations suggest that mitochondria are capable of responding to metabolic demand by first increasing OXPHOS efficiency then, if needed, increasing flux through OXPHOS, thus reflecting a novel and thermodynamically favorable paradigm of mitochondrial bioenergetics.

Key words: ATP/O ratio, mitochondrial function, ATP synthesis, permeabilized myofiber, oxidative phosphorylation, respiratory efficiency, uncoupling, adenylate kinase

INTRODUCTION

Dysfunction of mitochondrial oxidative phosphorylation (OXPHOS) has been implicated in the etiology of many diseases, including two leading causes of mortality: diabetes [86] and heart failure [87]. Although the two principle components of OXPHOS, ATP synthesis and respiration (i.e. O_2 consumption), can be measured individually, precisely how these two processes are integrated is critical to understanding if and how the efficiency of energetic coupling may be regulated at the sub-cellular level. OXPHOS efficiency is particularly important in highly oxidative tissues such as muscle, because conditions which cause supply-demand mismatches between oxygen delivery (i.e. blood flow) and oxygen demand (i.e. ATP turnover) are known to be core pathological features characteristic to metabolic and cardiovascular diseases. The ratio of ATP produced to atomic oxygen consumed, termed the ATP/O ratio, provides an index of mitochondrial efficiency but has proven difficult to measure. Experimentally generated ATP/O ratios have been reported for nearly sixty years with values ranging from 0.7 – 3.5 with NADH-linked substrates (reviewed by Hinkle [45]) but to date, no consensus values have been universally accepted. Further complicating matters, three notable limitations to previous approaches used to measure OXPHOS efficiency are that ATP synthesis rates are: 1) typically estimated based on ADP added [44, 88], 2) measured directly only at specific moments during an experimental protocol [89] and/or 3) usually only reported as a single level of metabolic demand (e.g. [ADP]). To circumvent these challenges, the purpose of this study was to develop and validate an approach to simultaneously measure ATP synthesis and O_2 consumption in real-time using PmFBs, similar to a recently described approach in isolated mitochondria [57].

In this report, we provide evidence that OXPHOS efficiency is a function of metabolic demand in PmFBs. Most notably, we have found that ATP synthesis can increase without a corresponding increase in JO_2, suggesting a decrease in proton leak and therefore, a greater proportion of Δp being used for ATP synthesis. Ultimately, based on these findings, the existing paradigm of mitochondrial bioenergetics may necessitate revision to include dynamic changes in OXPHOS efficiency as a function of metabolic demand.

EXPERIMENTAL PROCEDURES

Reagents. Hexokinase (HK) from yeast (Catalog #: 11426362001) and glucose-6-phosphate dehydrogenase (G6PDH) from *Leuconostoc mesenteroides* (Catalog #: 10165875001) were obtained from Roche Applied Science (http://www.roche-applied-science.com). All other chemicals and reagents were obtained from Sigma (http://www.sigma-aldrich.com).

Preparation of mouse permeabilized myofibers. All aspects of rodent studies were approved by the East Carolina University Animal Care and Use Committee. Male C57BL6/J mice were purchased from Jackson Laboratories. Mice were housed in a temperature- (22°C) and light-controlled room and given free access to food and water. At the time of experiment, mice were 8-12 weeks of age. The PmFB technique used was partially adapted from previous methods [90, 91] and has been described previously [92]. Mice were anesthetized by inhalation of isoflurane then euthanized by exsanguination and double pneumothorax, after which the left ventricle (LV), red (RG) and white portions of the gastrocnemius (WG) muscle were immediately excised. Muscle samples were placed in ice-cold (4°C) Buffer X containing (in mM): 7.23 K_2EGTA, 2.77 CaK_2EGTA, 20 Imidazole, 20 Taurine, 5.7 ATP, 14.3 Phosphocreatine, 6.56 $MgCl_2$-$6H_2O$ and 50 MES (pH 7.1, 295 mOsm). Under a dissecting microscope, fat and connective tissue were removed and muscle samples were separated into small bundles of fibers (<1 mg wet weight/fiber bundle). Fiber bundles were incubated in Buffer X supplemented

with 40 μg/ml saponin, a mild, cholesterol-specific detergent for 30 minutes as previously described [92]. PmFBs) were then washed in ice-cold Buffer Z containing (in mM): 110 K-MES, 35 KCl, 1 EGTA, 5 K_2HPO_4, 3 $MgCl_2$-$6H_2O$, and 5 mg/ml Bovine serum albumin (pH 7.4, 295 mOsm) and remained in Buffer Z on a rotator at 4°C until analysis (<4 hours). We have observed that mouse LV PmFBs exhibit EGTA-insensitive contraction that occurs even at 4°C (EJA and DSL, unpublished observations); therefore, 20 μM Blebbistatin was added to the wash buffer, in addition to the respiration medium, to mitigate the effects of contraction on respiratory kinetics [93].

Mitochondrial ATP production measurements. Illustrated in Figure 1A, *J*ATP was determined by coupling glucose-dependent, HK-catalyzed ATP hydrolysis to G6PDH-catalyzed reduction of $NADP^+$ to NADPH in a 1:1 stoichiometry [94]. To determine *J*ATP, O_2-equilibrated Buffer Z was supplemented with: 5 U/ml HK, 5 U/ml G6PDH, 5 mM D-Glucose and 5 mM nicotinamide adenine dinucleotide phosphate ($NADP^+$). Autofluorescence of NADPH was measured continuously at 30°C with 340/460 ex/em in a spectrofluorometer (FluoroMax-3, Horiba Jobin Yvon, Edison, NJ). Rates of ATP synthesis were quantified by generating standard curves with the enzyme coupled system based on the linear relationship between NADPH autofluorescence and ATP added (Figure 1B). Confirming the specificity of this assay for ATP synthesis, NADPH formation was not detectable in actively phosphorylating PmFBs in the absence of G6PDH (Figure 1C), the terminal enzyme of the assay system. Hereafter, the rate of NADPH accumulation is referred to as *J*ATP.

Simultaneous measurement of JO_2 and JATP in PmFBs. To generate quantitative ATP/O ratios in real-time from a single PmFB preparation, rates of oxygen consumption (JO_2) and *J*ATP were measured simultaneously using 2.5 ml of the assay buffer described above supplemented with 20 mM creatine monohydrate in a customized apparatus that combines a high-resolution respirometer (Oroboros O_2k, Innsbruck, Austria) with a monochromatic

spectrofluorometer (Photon Technology Instruments, Birmingham, NJ) (Figure 1D). A liquid light guide connected to the excitation monochromator was inserted into the respiration chamber of the O_2k through the top of the stopper. Another light guide was extended from the glass aperture of the respiration chamber directly into the emission detector of the spectrofluorometer.

Data Analysis and Calculations. Following the experimental protocol, PmFBs were removed from the chamber, rinsed in double distilled H_2O, lyophilized (Labconco, Kansas City, MO), and weighed using a precision calibrated scale (Orion Cahn C-35, Thermo Electron, Beverly, MA). For each step of the experimental protocol, JO_2 or *J*ATP data were obtained from identical time points and are reported as the mean of >20 seconds of steady-state data (>10 individual data points). Instrumental background rates (prior to any substrate additions) were subtracted from all subsequent values for JO_2 and *J*ATP and data were normalized to fiber dry weight. Final values are therefore reported as pmol O_2 consumed (or ATP produced) $\cdot sec^{-1} \cdot mg^{-1}$ dry wt for JO_2 and *J*ATP, respectively. ATP/O ratio was calculated by dividing the rate of ATP synthesis by the rate of atomic oxygen consumed using the following formula:

$$ATP/O = JATP/(JO_2*2)$$

Statistics. Data are presented as mean $\pm$ SEM unless otherwise noted. Statistical analyses were performed using one-way analysis of variance (ANOVA) with Student-Newman-Keuls, two-way ANOVA with Bonferroni post-hoc testing or Student's two-way unpaired t-test to determine significance between groups where appropriate. The level of significance was set at $p < 0.05$.

Results and Discussion

ATP/O ratio kinetics in permeabilized myocardium, oxidative and glycolytic skeletal muscle. A representative trace showing an increase in JO_2 and *J*ATP as a function of [ADP] is

provided in Figure 2. *J*ATP and JO_2 were both greater in myocardium and oxidative skeletal muscle compared to glycolytic skeletal muscle (Figures 3A and B), consistent with established differences in mitochondrial content between these tissue types. The Pearson correlation coefficients for *J*ATP at a given JO_2 were strong ($r^2 > 0.8$) in all three tissues (Figure 3C), suggesting that corresponding changes in *J*ATP and JO_2 measured with this approach reflect demand-driven flux through OXPHOS.

ATP/O ratios were lower in LV than WG at 20 and 75 μM ADP but not overall and not between RG and LV or WG (Figure 4A). ATP/O ratio reached maximal levels between 75 and 200 μM ADP in all three tissues, and did not differ among groups (Figure 4B). These differences in OXPHOS efficiency kinetics between tissues are particularly intriguing because the kinetics of O_2 consumption are slower in heart than in skeletal muscle PmFBs [90] while ATP/O ratio kinetics in skeletal muscle are similar between this study and a recent report in isolated rat hindlimb muscle mitochondria [57]. The similarities in OXPHOS efficiency kinetics between preparations but not between tissues suggests the electron transport system components are conserved across tissues and that extramitochondrial mechanism(s) likely contribute to the varying degrees of OXPHOS affinity for ADP and OXPHOS efficiency.

A classic and pervasive dogma in mitochondrial physiology is that metabolic demand requires increased O_2 flux to support greater rates of ATP synthesis and is supported by over 60 years of seminal research. The data presented here reveal that ATP/O ratio increases as a function of ADP added in both myocardium and skeletal muscle (Figure 4A, $p<0.0001$), an observation that is supported by comparable data recently reported using isolated mitochondria from rat liver and skeletal muscle [57]. Ultimately, if OXPHOS efficiency increases as a function of metabolic demand, then it implies that the mitochondrion possesses an energy conserving mechanism to support metabolic demand.

The advantage of demand-driven enhancement of OXPHOS efficiency is readily apparent when considering that maximal oxygen consumption (VO_{2max}) *in vivo* is limited by O_2 diffusion into skeletal muscle (cite Roca et al. 1989) and thus O2 availability (Hogan 1994 and others). Furthermore, O2 consumption increases as a function of contraction frequency in isolated skeletal muscle fibers (cite Hogan's work). Altogether, the ability of the mitochondrion to maximize the efficiency of energy production would allow for greater work to be performed at a given rate of O2 consumption.

Consistent with dynamic OXPHOS efficiency being a potentially requisite aspect of the mitochondrial response to metabolic demand, the data provided suggest that PmFBs can increase ATP synthesis and OXPHOS efficiency apparently independent of an increase in O_2 flux (5 and 20 μM ADP additions compared to 0 ADP added in Figures 4A, 4B and 5A). Alternatively stated, these data suggest that the initial response of mitochondria to metabolic demand may be remodeling of proton conductance that favors ATP synthesis over proton leak. Since 20 μM corresponds to the [ADP] required to reach half-maximal respiratory capacity in isolated mitochondria [57], the observation that *J*ATP increases independent of JO_2 at 20 μM ADP appears to be unique to PmFBs. This may explain why PmFBs display an elevated rate of "basal" respiration compared with mitochondria isolated by differential centrifugation [95]. Regardless, these data altogether reveal a novel mechanism of mitochondrial adaptation to metabolic demand that necessitates a model (PmFBs in the presence of contraction inhibitors) that is better aligned with respiratory kinetics found *in vivo*.

Mechanistic vs. Experimental ATP/O ratios. Although the theoretical maximum, or "mechanistic", ATP/O ratio is constantly being revised as new information regarding the thermodynamics of proton pumping and ATP synthesis are being disseminated, a current

mechanistic ATP/O ratio for pyruvate/malate supported OXPHOS can be generated based on the following calculations: 4 H^+ are pumped from Complex I [51], 2 H^+ from Complex III [52] and 4 H^+ from Complex IV [53] per NADH oxidized. A single H^+ is used to import pyruvate to the mitochondrial matrix [96], and since 3 NADH are generated from the metabolism of pyruvate and malate through the TCA cycle, 0.33 H^+ must be subtracted from the protons pumped from pyruvate oxidation, yielding 9.67 H^+ per NADH. A recent study, the first in mammalian ATP synthase, suggests that 2.7 H^+ are required to synthesize ATP [55]. The electrogenic exchange of ADP + P_i for ATP across the inner membrane via adenine nucleotide translocase (ANT) adds an additional H^+ to the bioenergetic cost of making ATP, which overall yields an H^+/ATP ratio of 9.67/3.7 for pyruvate/malate-supported ATP synthesis, and therefore a mechanistic ATP/O ratio of 2.61. The differences accounting for the differences between the mechanistic ATP/O ratio and our reported experimental ATP/O ratios are unknown but may be attributed to proton leak and/or slip, although the latter remains controversial and possibly diminutive [49]. Sources of mitochondrial proton leak include ANT [37, 97] and possibly uncoupling proteins (UCPs), namely UCP3 in heart and skeletal muscle [31, 34, 98], however, the latter is activated by fatty acids [31, 34] and reactive oxygen species (ROS) [99]. Neither fatty acids or ROS are likely mediators under the conditions tested though, since 5 mg/ml BSA was present to chelate free fatty acids and ROS levels are low with pyruvate and malate under both state 3 and state 4 conditions unless glutathione is removed from mitochondria [3]. ANT is of particular interest since it could, at a constant rate of proton conductance, serve as a source of proton leak or adenine nucleotide exchange based on the needs of the cell, consistent with the finding that *J*ATP and ATP/O ratios increase without a corresponding increase in the number of protons pumped (e.g. no increase in JO_2). Altogether, the data presented suggest that the mitochondrion is capable of greatly altering its intrinsic bioenergetic properties in response to metabolic demand; however, even at experimentally maximal OXPHOS efficiency, >20% of O_2 consumption may still contribute to thermogenesis. How this adaptation to OXPHOS efficiency

occurs through ANT or elsewhere will be central to furthering our understanding of mitochondrial bioenergetics and OXPHOS efficiency.

Adenylate kinase as a source of ATP synthesis in PmFBs. While OXPHOS is the primary source of ATP production in aerobic cells and organisms, other sources of ATP production exist (e.g. adenylate kinase (AK). Since isozymes of AK have been detected in both rodent cardiac [100] and skeletal muscle PmFBs [101], it was hypothesized that AK would be a detectable source of ATP production in PmFBs. To test this hypothesis, ATP synthesis was determined in LV, RG and WG in the absence of respiratory substrates following the addition of 75 μM ADP. Under these conditions, the addition of ADP generated detectable rates of ATP synthesis in all three tissues (Figures 5A-C). Consistent with this ATP production being independent of OXPHOS, rates were also detected in the presence of the ATP synthase inhibitor oligomycin in the presence of the ANT inhibitor carboxyatractylate, suggesting that the source of ATP production was at least in part from outside the mitochondrial matrix. The addition of 200 μM diadenosine pentaphosphate (Ap5A), an AK inhibitor [102], essentially abolished *J*ATP in all tissues under all conditions. Altogether, these data support adenylate kinase as an OXPHOS-independent source of ATP production in permeabilized mouse cardiac and skeletal muscle myofibers. Notably, Ap5A did not alter the sensitivity of the enzyme-coupled ATP detection system (data not shown).

To determine whether AK influences ATP/O ratios, JO_2 and *J*ATP were measured simultaneously in LV, RG and WG in the absence or presence of 200 μM Ap5A. Ap5A treatment decreased ATP/O ratios at higher [ADP] in LV (Figure 6A), but not RG (Figure 6B) or WG (Figure 6C). Notably, the inhibition of AK did not alter the [ADP]-dependent increase in ATP/O ratio observed previously. These data indicate that AK should be accounted for when measuring ATP/O ratio kinetics in myocardium; however, since intracellular ATP is present in

millimolar concentrations, the findings here should not be interpreted as potential differences in AK function *in vivo*.

A New Paradigm of Mitochondrial Bioenergetics. In this report, we provide the first direct evidence that metabolic demand elicits an increase in OXPHOS efficiency that precedes increased absolute flux through OXPHOS. This finding is particularly important given the wide dynamic range of [ADP] in skeletal muscle (5 - 500 μM) from rest to maximal exercise [103, 104]and may serve to provide a better understanding of exercise tolerance and even the functional impact of acute and chronic adaptations to exercise training. In contrast, it has been previously established that myocardial [ADP] is relatively static regardless of workload [105] and for this reason, ADP-dependent changes in OXPHOS efficiency may not be physiologically relevant in the heart. Parenthetically, we have recently demonstrated that contraction inhibitors (e.g. blebistatin) elucidate respiratory kinetics in PmFBs that are line with fluctuations in mitochondrial dynamics *in vivo* [93]. In the current report, contraction inhibitors were used in PmFBs to provide experimental ATP/O ratios across a physiologically relevant range of ADP concentrations. Paramount of these findings is that ATP synthesis rates and OXPHOS efficiency appear to increase independent of increased O_2 flux, a finding that would fail to be realized based on the established respiratory kinetics of both isolated mitochondria and perhaps even PmFBs in the absence of contraction inhibitors [93]. Ultimately, we contend that the findings reported here were only made possible by, and are also limited by, using this recently described strategy for measuring mitochondrial bioenergetics.

In this revised model of mitochondrial bioenergetics, depicted in Figure 7, the physiological role of skeletal muscle mitochondria within the organism during the transition from rest to metabolic demand shifts from a largely thermogenic system operating at a low OXPHOS efficiency to one that is committed to generating ATP, at least in part by increasing ATP/O ratio. Importantly, despite this effort to optimize OXPHOS efficiency, under the conditions tested here, skeletal

muscle PmFBs oxidizing pyruvate and malate are still <80% efficient based on the currently accepted mechanistic ATP/O ratio; therefore, our findings suggest that >20% of O_2 consumption is still attributed to thermogenic proton leak. Given the exponential increase in OXPHOS flux required to produce sufficient ATP under levels of high metabolic demand, it is likely that overall thermogenesis is increased under high levels of metabolic demand despite a decrease in proton leak per O_2 consumed. Nonetheless, the findings reported here provide a new conceptual framework for mitochondrial physiology and suggest that the mitochondrion acts like a motor vehicle in that an idling engine is not only running, but is running at a level sufficient to move the vehicle, albeit probably at a slow speed (e.g. when the brake is released).

Ultimately, the primary finding was that OXPHOS efficiency increased as a function of the amount of ADP added. This observation is consistent with a recent report in isolated rat skeletal muscle mitochondria [57] using a similar technique and measurements in permeabilized human atrium using the technique described here [113], altogether suggesting that demand-driven enhancement of OXPHOS efficiency may be a conserved bioenergetic response across all eukaryotic species. If confirmed, this would be of profound importance, since muscular work *in vivo* is thought to be in large part limited by O_2 diffusion into tissues [134, 135]. Therefore, demand-driven enhancement of OXPHOS efficiency would represent a fundamental physiological mechanism allowing mitochondria to maximize ATP production at a given rate of O_2 flux and have relevance in every mitochondrion-containing tissue.

Conclusions

The current study has described a novel approach to quantify OXPHOS efficiency as a function of metabolic demand and, in doing so, revealed that mitochondrial OXPHOS efficiency increases as a function of metabolic demand. This increase in OXPHOS efficiency precedes increased absolute flux through OXPHOS measured as JO_2 and therefore, suggests a new

paradigm of mitochondrial physiology that involves enhancement of OXPHOS efficiency as a response to metabolic demand that precedes increased O_2 consumption. The implications of this observation are diverse and may universally improve our understanding of cellular metabolism.

Figure 1. Assay Chemistry, Instrumentation and Validation. A) Determination of ATP production is achieved through enzyme-coupled phosphorylation and subsequent oxidation of glucose, consuming ATP and generating NADPH. NADPH autofluorescence was detected at 340/460 ex/em. **B)** Fluorescence was measured through a randomized fiber optic cable inserted into the air-tight, volume calibrated respirometer chamber. **C)** Titration of known amounts of ATP yielded linear increases in NADPH autofluorescence. N=3 independent observations. **D)** In the absence of G6PDH, the terminal enzyme of the assay system described in Figure 1A, actively phosphorylating mitochondria do not generate a detectable amount of NADPH. Upon addition of G6PDH, accumulated ATP is hydrolyzed then a steady-state rate of ATP production continues.

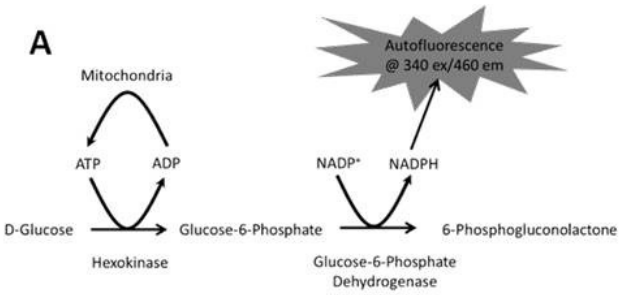
A
Mitochondria
ATP
ADP
D-Glucose
Hexokinase
Glucose-6-Phosphate
Autofluorescence
@ 340 ex/460 em
NADP+
NADPH
Glucose-6-Phosphate
Dehydrogenase
6-Phosphogluconolactone


B

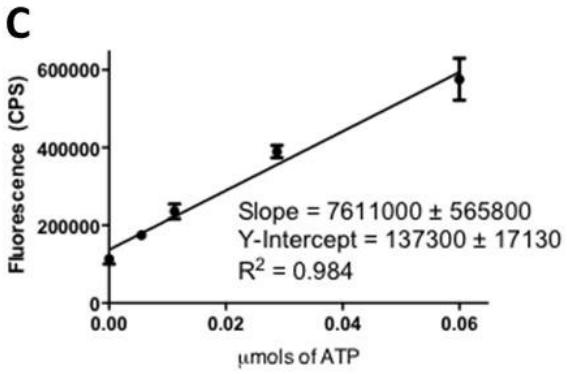
C
Fluorescence (CPS)
600000
400000
200000
0
0.00
0.02
0.04
0.06
µmols of ATP
Slope = 7611000 ± 565800
Y-Intercept = 137300 ± 17130
R2 = 0.984

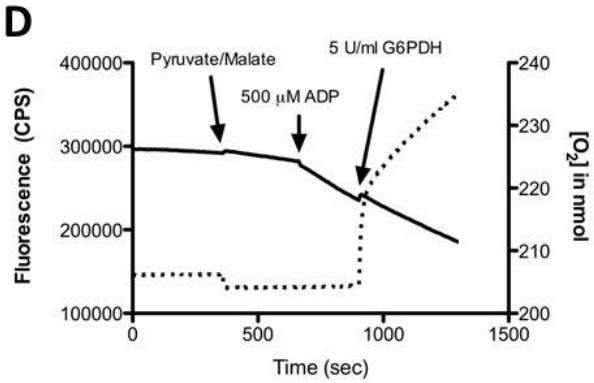
D
Fluorescence (CPS)
400000
300000
200000
100000
0
500
1000
1500
Time (sec)
Pyruvate/Malate
500 µM ADP
5 U/ml G6PDH
[O2] in nmol
240
230
220
210
200

Figure 2. A representative experiment performed to determine OXPHOS efficiency kinetics. NADPH autofluorescence (left Y-axis, solid line) and [O_2] (right Y-axis, dashed line) were measured simultaneously in a single sample using the apparatus pictured in Figure 1B. The addition of NAD^+-linked respiratory substrates (pyruvate/malate) elicited an increase in O_2 consumption, but not ATP synthesis, reflecting state 4 "leak-dependent" respiration. The addition of ADP dose-dependently increased both O_2 consumption and ATP synthesis, reflecting the coordination necessary for OXPHOS to support increasing metabolic demand.

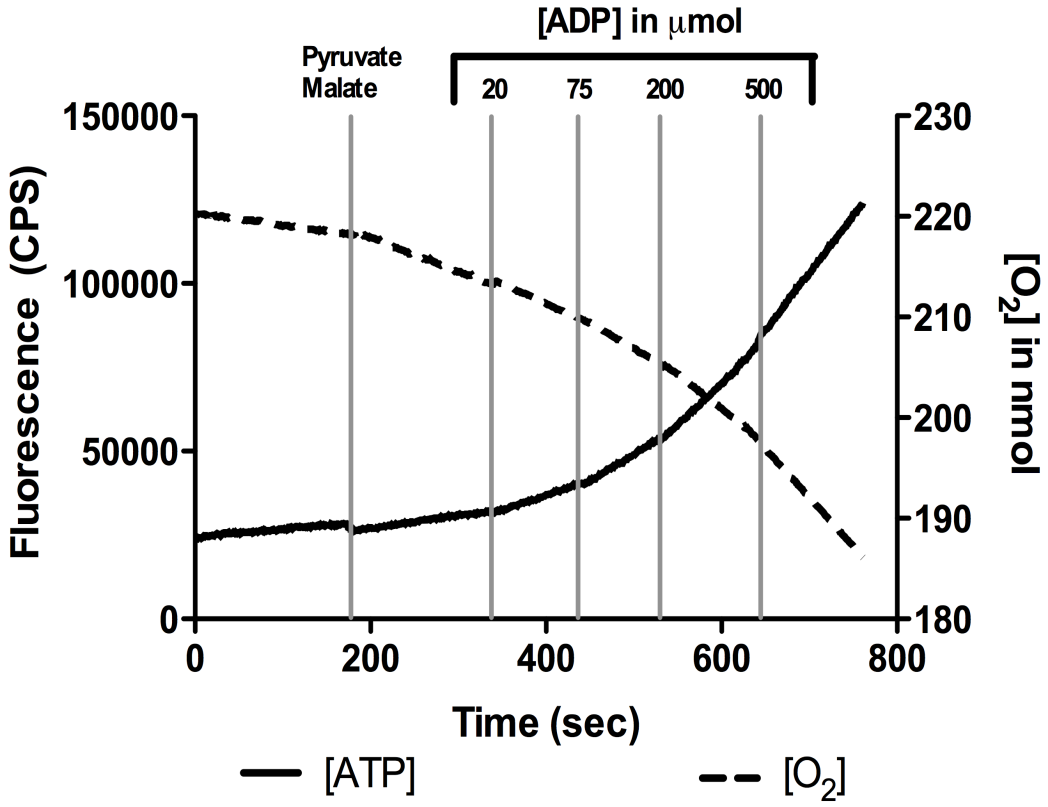
[ADP] in μmol
Pyruvate
Malate
20
75
200
500
150000
100000
50000
0
Fluorescence (CPS)
230
220
210
200
190
180
[O2] in nmol
0
200
400
600
800
Time (sec)
[ATP]
[O2]

Figure 3: Rates of ATP synthesis and O_2 consumption measured as a function of metabolic demand in PmFBs. Rates of ATP synthesis (*J*ATP) (**A**) and O_2 consumption (JO_2) (**B**) were measured in left ventricle (LV), red gastrocnemius (RG) and white gastrocnemius (WG) during ADP titration experiments as described in Figure 2. Pearson correlation coefficients were determined for *J*ATP as a function of JO_2 in LV (**C**), RG (**D**) and WG (**E**). N=6-10 per condition. * denotes $p<0.05$ compared to LV, Ψ denotes $p<0.05$ compared to RG.

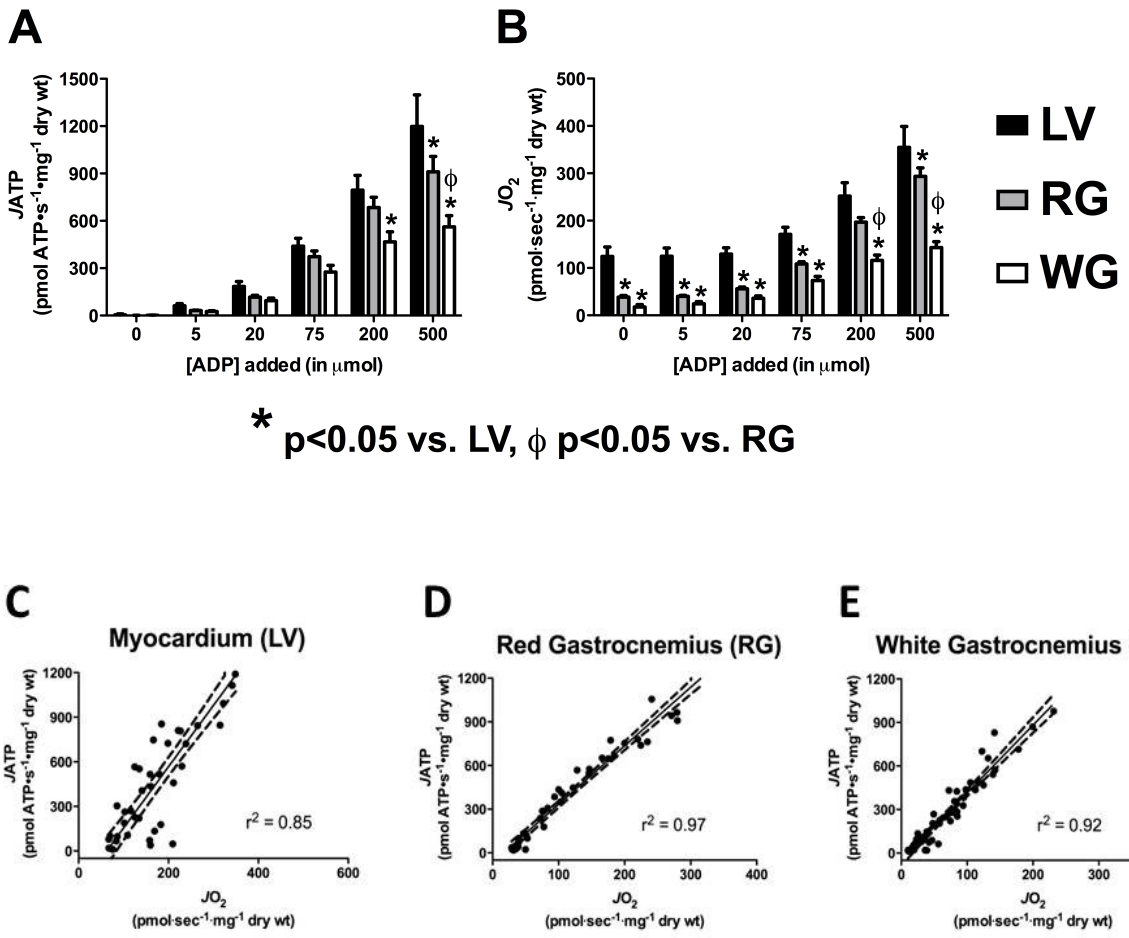
A
B
JATP
(pmol ATP•s-1•mg-1 dry wt)
JO2
(pmol•sec-1•mg-1 dry wt)
[ADP] added (in μmol)
LV
RG
WG
* p<0.05 vs. LV, ϕ p<0.05 vs. RG
C
Myocardium (LV)
D
Red Gastrocnemius (RG)
E
White Gastrocnemius (WG)
r2 = 0.85
r2 = 0.97
r2 = 0.92

Figure 4: OXPHOS Efficiency as a function of metabolic demand in PmFBs. **A**) ATP/O ratio was determined in LV (black bars), RG (gray bars) and WG (white bars) as a function of ADP added. **B**) The maximal ATP/O ratio at a given ADP for each experiment averaged for LV (black bars), RG (gray bars) and WG (white bars). N=6-10/tissue. * denotes $p<0.05$ compared to LV.

A

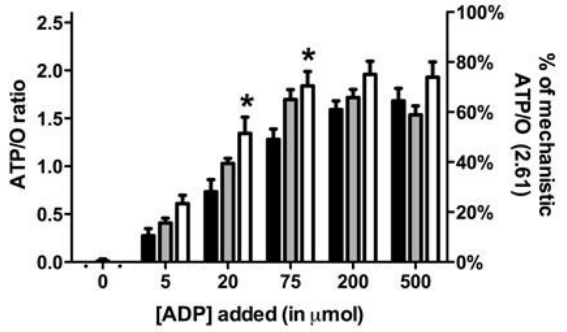

Main effect of [ADP] p<0.0001

B

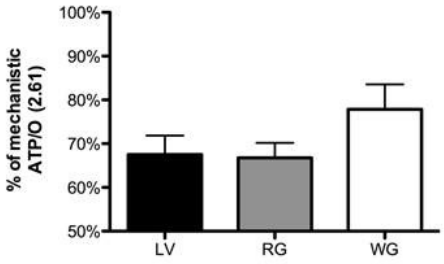

	LV	RG	WG
Mean	67.53	66.78	77.85
Std. Deviation	12.21	9.626	18.04
Std. Error	4.316	3.403	5.704

Figure 5: Adenylate kinase is a source of ATP production in PmFBs. *J*ATP was detected in LV (A), RG (B) and WG (C) in the presence of 75 μM ADP, the absence of respiratory substrates (black bars) and in the presence of oligomycin (gray bars) or carboxyatractylate (white bars) to inhibit ATP synthase or ANT, respectively. The subsequent addition of 200 μM Ap5A (adjacent bar in each tissue/condition test) inhibit adenylate kinase abolished *J*ATP under every condition tested. N=3-4/condition, N.D. = not detectable.

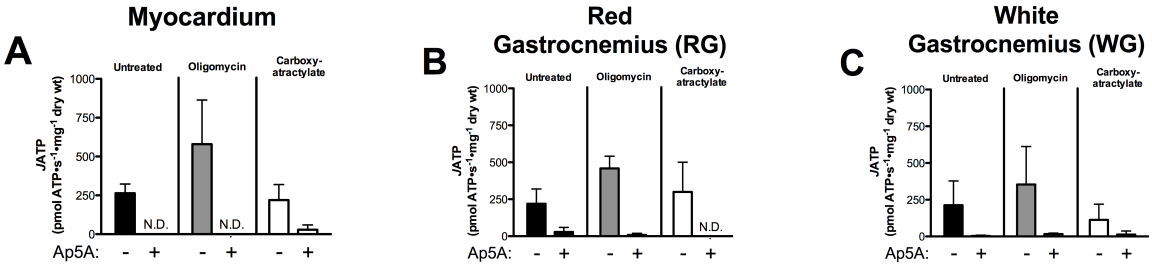
A
Myocardium
Untreated
Oligomycin
Carboxy-
atractylate
JATP
(pmol ATP•s-1•mg-1 dry wt)
1000
750
500
250
0
N.D.
N.D.
Ap5A: - + - + - +
B
Red
Gastrocnemius (RG)
Untreated
Oligomycin
Carboxy-
atractylate
JATP
(pmol ATP•s-1•mg-1 dry wt)
1000
750
500
250
0
N.D.
Ap5A: - + - + - +
C
White
Gastrocnemius (WG)
Untreated
Oligomycin
Carboxy-
atractylate
JATP
(pmol ATP•s-1•mg-1 dry wt)
1000
750
500
250
0
Ap5A: - + - + - +

Figure 6: Effects of AK inhibition of ATP/O ratio in PmFBs. ATP/O ratio was measured in absence (white bars) or presence (black bars) of 200 μM Ap5A to inhibit AK in LV (A), RG (B) or WG (C). N=6-10/condition. * denotes $p<0.05$ compared to untreated condition.

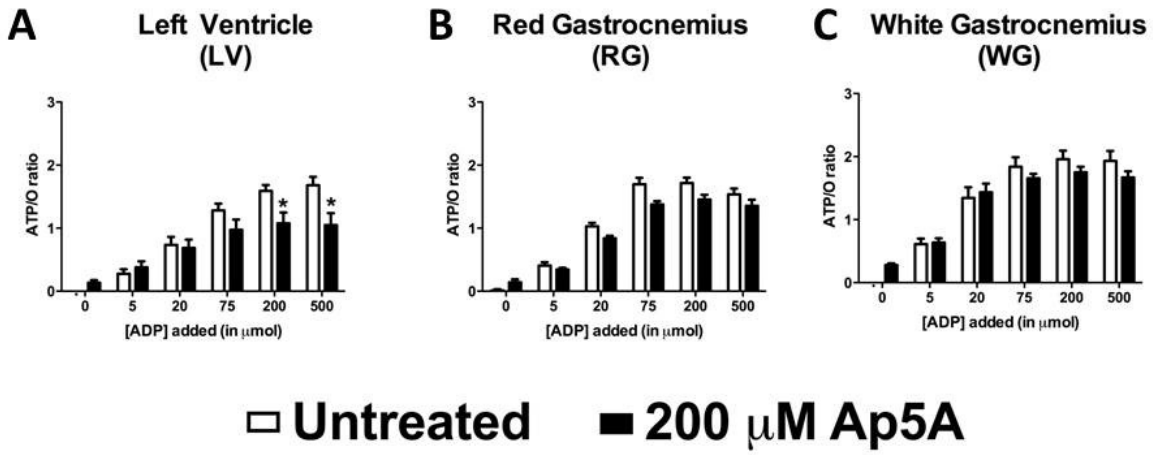
A
Left Ventricle
(LV)
B
Red Gastrocnemius
(RG)
C
White Gastrocnemius
(WG)
ATP/O ratio
[ADP] added (in μmol)
0
5
20
75
200
500
*
Untreated
200 μM Ap5A

Figure 7: A working hypothesis for demand-driven enhancement of OXPHOS efficiency. Endothermic organisms rely on mitochondria for non-shivering thermogenesis via proton leak (red line) and for maintaining energy homeostasis via ATP production. As metabolic demand increases, the data provided indicate that OXPHOS efficiency, defined as the ATP/O ratio (green line), increases. Since protonmotive force is consumed by ATP synthesis and proton leak, increased ATP/O ratio implies a corresponding decrease in proton leak. Altogether, the working hypothesis provided posits that, in response to metabolic demand, protonmotive force is preferentially used for ATP synthesis in an effort to maintain energy homeostasis at the lowest possible rate of O_2 flux.

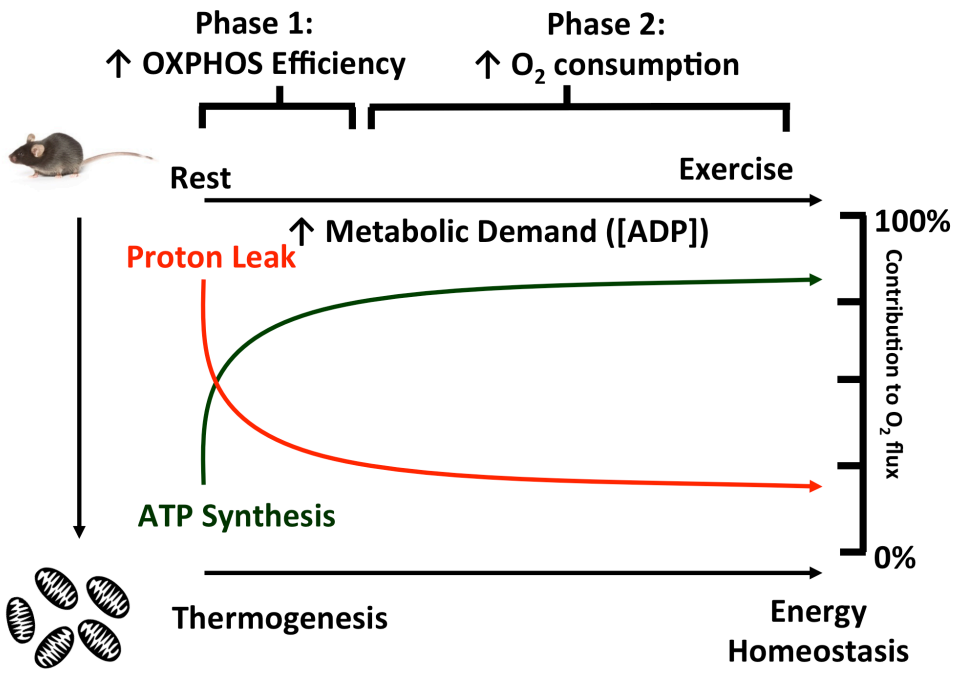
Phase 1:
↑ OXPHOS Efficiency
Phase 2:
↑ O_2 consumption
Rest
Exercise
↑ Metabolic Demand ([ADP])
Proton Leak
ATP Synthesis
100%
0%
Contribution to O_2 flux
Thermogenesis
Energy
Homeostasis

CHAPTER 3: PKA ACTIVITY GOVERNS OXIDATIVE PHOSPHORYLATION KINETICS AND OXIDANT EMITTING POTENTIAL AT COMPLEX I IN PERMEABILIZED MYOFIBERS

Daniel S. Lark[1,3], Lauren R. Reese[2,3], Terence E. Ryan[2,3] and P. Darrell Neufer[1,2,3].

Departments of [1]Kinesiology, [2]Physiology, [3]and East Carolina Diabetes and Obesity Institute, East Carolina University, Greenville, North Carolina

Running Head: ATP/O in permeabilized mouse and human myofibers

† To whom correspondence should be addressed:

P. Darrell Neufer (NEUFERP@ECU.EDU) Department of Physiology, East Carolina University, East Carolina Heart Institute, Room 4101, 115 Heart Dr., Greenville NC 27834

SUMMARY

Oxidative phosphorylation (OXPHOS) is a dynamic machine that not only produces ATP but also participates in redox-dependent cell signaling. Reversible phosphorylation of mitochondrial proteins, particularly via the cyclic AMP (cAMP)/Protein kinase A (PKA) axis, has been revealed as a basic mechanism of regulation of OXPHOS, but the interplay between substrate oxidation and regulation of OXPHOS is incompletely understood. In this report, we provide evidence that endogenous TCA cycle flux is insufficient to activate the mitochondrial cAMP/PKA axis and that supra-physiological levels of cAMP do not enhance respiratory capacity. In permeabilized myofibers (PmFBs), PKA regulates OXPHOS via phosphorylation of Complex I between the flavin (F) and quinone (Q) sites of electron transfer, possibly at the 18kDa subunit of Complex I, a known site of PKA-mediated phosphorylation. Summarily, these data reveal Complex I as a primary target of the mitochondrial cAMP/PKA axis that is capable of inhibiting flux through OXPHOS.

HIGHLIGHTS:

1) Endogenous TCA cycle flux is insufficient to increase mitochondrial [cAMP].

2) Supra-physiological levels of cAMP do not increase maximal respiratory capacity.

3) PKA regulates respiratory kinetics via Complex I of the ETS.

INTRODUCTION

Evidence is mounting implicating post-translational modifications to mitochondrial proteins, particularly phosphorylation events mediated by the cyclic AMP (cAMP) / Protein kinase A (PKA) axis, as a key form of regulation of cellular metabolism [106, 107]. Central to these recent developments, the MitoCarta [108] has provided a comprehensive database outlining phosphorylation of the entire mitochondrial proteome. Subsequent studies utilizing the Mitocarta have revealed up to 75 different mitochondrial proteins that are putative targets of PKA-mediated phosphorylation, some of which are altered by dietary manipulation [76]. In addition to the Mitocarta database, a number of independent groups have also identified Complex I of the electron transport system (ETS), particularly the 18kDa (or AQDQ) subunit, as a target of PKA-dependent phosphorylation [79, 81], altogether implicating Complex I defects in a number of human pathologies [82, 109]. Despite the mounting evidence implicating Complex I deficiency as a central component of numerous human diseases, the direct functional relevance of Complex I phosphorylation in the context of mitochondrial bioenergetics is incompletely understood.

The mitochondrial cAMP/PKA axis is reported to be, at least in part, governed by soluble adenylyl cyclase [60], a bicarbonate-activated [64] source of cAMP that has been found in the mitochondrial matrix [110], as well as other cellular compartments (e.g. nucleus). Further studies into sAC function ultimately led to reports demonstrating that cAMP/PKA signaling within the mitochondrial matrix can alter oxidative phosphorylation (OXPHOS) by regulating cytochrome C oxidase [67, 84, 85] or modulating ATP production in the presence of Ca^{2+} [62]. However, despite the preponderance of evidence demonstrating that mitochondrial sAC can be activated via exogenous bicarbonate, it is not known whether endogenous sources of

bicarbonate production (e.g. flux through the tricarboxylic acid (TCA) cycle) increases cAMP levels within mitochondria. Addressing these issues, we hypothesized that: 1) CO_2 production from the TCA cycle will be sufficient to increase mitochondrial cAMP levels and 2) PKA acts on multiple ETS complexes (including Complex I) to ensure that oxidative phosphorylation is primed to respond to metabolic demand but does not digress from chemiosmotic theory.

In this report, we provide evidence that endogenous TCA cycle flux alone is insufficient to increase steady-state cAMP levels, suggesting that additional co-activators (e.g. Ca^{2+} and/or other divalent cations) may be necessary to drive cAMP production via sAC. Furthermore, we have found that commonly used inhibitors of soluble adenylyl cyclase (KH7 and 2-hydroxyestradiol) have distinct off-target effects that may preclude their use when studying mitochondrial bioenergetics. We demonstrate that exogenous addition of a membrane-permeable cAMP mimetic does not increase mitochondrial respiratory capacity in isolated liver mitochondria, suggesting that the cAMP/PKA axis is maximally activated during oxidative phosphorylation. Finally, we demonstrate that a pharmacological inhibitor of PKA decreases Complex I, but not Complex II, supported respiration. Furthermore, pharmacological inhibition of PKA decreased oxidation of pyruvate and glutamate, as well as electron leak from Complex I is decreased in the reverse, but not forward, direction. These effects occurred independent of a decrease in the efficiency of oxidative phosphorylation efficiency. Therefore, our data collectively suggest that pharmacological inhibition of PKA results in disruption of electron flow between the flavin and quinone sites of Complex I, possibly at the 18 kDa accessory subunit of Complex I, an established target of PKA-dependent phosphorylation.

METHODS

Chemicals and Reagents. Hexokinase (HK) from yeast (Catalog #: 11426362001) and glucose-6-phosphate dehydrogenase (G6PDH) from *Leuconostoc mesenteroides* (Catalog #: 10165875001) were obtained from Roche Applied Science (http://www.roche-applied-science.com). All other chemicals and reagents were obtained from Sigma (http://www.sigma-aldrich.com).

Mitochondrial Isolation. All aspects of rodent studies were approved by the East Carolina University Animal Care and Use Committee. Male C57BL6/NJ mice were purchased from Jackson Laboratories. Mice were housed in a temperature- (22°C) and light-controlled room and given free access to food and water. At the time of experiment, mice were 8-12 weeks of age. Mice were anaesthetized by inhalation of isoflurane then euthanized by exsanguination and double pneumothorax, after which the liver or hindlimb muscle (gastrocnemius, quadriceps and biceps femoris) were immediately excised and mitochondria were isolated using differential centrifugation.

Mitochondrial cAMP Production Assay. To determine steady-state cAMP levels following the addition of various substrates and inhibitors, skeletal muscle mitochondria (250 µg/ml) were incubated for 10 minutes at 37°C in 300 µl of MAITE medium containing (in mM): 10 Tris-HCl, 25 sucrose, 75 sorbitol, 100 KCl, 0.5 EDTA, 5 $MgCl_2$ and 1 mg/ml BSA; pH 7.4, supplemented with 1 mM ATP and in the presence or absence of inhibitors of sAC (25 µM KH7) or carbonic anhydrase (CA) (5 µM acetazolamide (AZA)). Following the initial incubation period, samples were incubated with respiratory substrates according to specific CO_2 generating stoichiometries: 5 mM pyruvate/ 2mM Malate, 5 mM succinate or 25 µM palmitoyl-carnitine/2 mM malate for an additional 5 minutes then in the presence or absence of 1 µM FCCP to uncouple O_2

consumption from ATP synthesis and thereby accelerate flux through the TCA cycle. A separate set of control samples did not receive respiratory substrates. Immediately following the incubation period, 200 µl of 0.1 M HCl were added to samples, which were then briefly vortexed and flash frozen in liquid N_2. Samples were thawed, vortexed then cAMP was measured using a commercially available kit as described (Complete cAMP ELISA Kit, Enzo Life Sciences)

Preparation of Mouse Permeabilized Myofibers. The PmFB technique used was partially adapted from previous methods [90, 111] and has been described previously [92]. Mice were anaesthetized by inhalation of isoflurane and the red (RG) and white (WG) portions of the gastrocnemius muscle were immediately excised with animals being euthanized by double pneumothorax. Muscle samples were placed in ice-cold (4°C) Buffer X containing (in mM): 7.23 K_2EGTA, 2.77 CaK_2EGTA, 20 Imidazole, 20 Taurine, 5.7 ATP, 14.3 Phosphocreatine, 6.56 $MgCl_2$-$6H_2O$ and 50 MES (pH 7.1, 295 mOsm). Under a dissecting microscope, fat and connective tissue were removed and muscle samples were separated into small bundles of fibers (<1 mg wet weight/fiber bundle). Fiber bundles were incubated in Buffer X supplemented with 40 µg/ml saponin, a mild, cholesterol-specific detergent for 30 minutes as previously described [92]. Since the sarcolemmal membrane contains a large amount of cholesterol relative to the mitochondrial membrane, this technique selectively permeabilizes the sarcolemma while leaving mitochondrial membranes and ultra-structure intact [46]. Permeabilized myofiber bundles (PmFBs) were then washed in ice-cold Buffer Z containing (in mM): 110 K-MES, 35 KCl, 1 EGTA, 5 K_2HPO_4, 3 $MgCl_2$-$6H_2O$, and 0.5 mg/ml Bovine serum albumin (pH 7.4, 295 mOsm) and remained in Buffer Z on a rotator at 4°C until analysis (<4 hours).

Mitochondrial Bioenergetics Assays. Mitochondrial respiration experiments in both isolated mitochondria and PmFBs were performed using a high-resolution oxygraph (Oroboros O_2k, Innsbruck Austria). Isolated mitochondria experiments were performed in Buffer Z at 25°C while substrate titration experiments in PmFBs were performed at 37°C in Buffer Z supplemented with 20 mM creatine monohydrate to maximize phosphate transfer in PmFBs [90] and 20 μM Blebbistatin to mitigate the effects of contraction on respiratory kinetics [93] as previously described [112]. Simultaneous detection of ATP synthesis and O_2 consumption was performed at 30ºC using a custom-designed oxi-fluorimeter as recently described [113].

Mitochondrial oxidant emitting potential (mOEP), defined as the H_2O_2 that escapes the matrix, was determined by measuring the fluorescence accumulation of Amplex Ultra Red (Invitrogen) at 565/600 ex/em at 37°C in a monochromatic spectrofluorometer (Horiba Jobin-Yvon) with Buffer Z as previously described [92]. Assays were performed in the presence of 25 U/ml superoxide dismutase to ensure rapid and complete conversion of superoxide to H_2O_2. mOEP was measured as either reverse electron flow using 5 mM succinate or forward electron flow using 5 mM glutamate and 2 mM malate followed by the addition of rotenone [114]. Following a steady-state rate of H_2O_2 emission being established (< 10 minutes), 1 μM auranofin, a thioredoxin reductase inhibitor, was added to inhibitor endogenous oxidant scavenging and thereby allow for the determination of H_2O_2 producing potential (mOPP) [3] and deductively, an index of mitochondrial scavenging capacity (scavenging potential = mOPP - mOEP).

Statistical Analyses

Comparisons between control and treatment groups were made using one-way ANOVA with Student Newman-Keuls post-hoc test where appropriate using Prism statistical software

(GraphPad Prism 6). Pair-wise comparisons were made using student's paired t-test. In all experiments, data are reported as mean ± SD unless otherwise noted. Significance level was set a $p<0.05$.

RESULTS

TCA cycle flux is insufficient to increase [cAMP] in isolated mitochondria.

Exogenous bicarbonate increases cAMP levels in mitochondria [61, 62, 64, 110](Supplemental Figure 1A). To determine if endogenous TCA cycle flux through CO_2-producing (e.g. pyruvate, isocitrate and α-ketoglutarate) dehydrogenases also increases mitochondrial cAMP levels, isolated skeletal muscle mitochondria were incubated in the presence of respiratory substrates that produce CO_2 (e.g. pyruvate and malate) or substrate conditions that do not generate CO_2 (succinate). Furthermore, to determine the contribution of sAC or carbonic anhydrase, parallel experiments were performed in the presence of KH7 or acetazolamide, inhibitors of sAC [115] and carbonic anhydrase [116], respectively. Finally, parallel experiments were also performed in the presence of FCCP, a mitochondrial uncoupler [117], to maximize TCA cycle flux and therefore, CO_2 production. To ensure adequate substrate for cAMP production, all experiments were performed in the presence of 1 mM ATP. Surprisingly, TCA cycle flux supported by pyruvate/malate did not increase cAMP levels in the absence or presence of FCCP compared with mitochondria in the absence of respiratory substrates or in the presence of succinate (Figure 1A). In addition to a lack of TCA cycle-dependent changes in cAMP levels, no effect of KH7 or AZA was observed, suggesting that alternative pathways may be responsible for the basal level of cAMP detected under these experimental conditions.

Available evidence to date suggests cAMP is locally produced and does not cross membranes; however, there is conflicting evidence regarding whether exogenously activating PKA increases [67] or decreases [62] mitochondrial ATP production. In this study, we determined the effect of

an exogenous increase in PKA activity on mitochondrial respiratory capacity using distinct protocols designed to exclusively measure O_2 flux supported by Complex I (glutamate/malate) or Complex II (succinate/rotenone) in isolated liver mitochondria in the absence or presence of 1 mM 8-Br-cAMP, a membrane-permeable cAMP mimetic. Following the addition of ADP to stimulate maximal phosphorylating respiration, cytochrome c was added to assess the integrity of mitochondrial membranes, then FCCP to determine maximal uncoupled respiration. In the presence of 8-Br-cAMP, ADP-stimulated respiration with glutamate/malate was decreased but leak-dependent respiration was unchanged compared to untreated mitochondria (Figure 1B). These differences in ADP-stimulated respiration were retained in the presence of cytochrome C and FCCP, suggesting that 8-Br-cAMP did not alter mitochondrial membrane integrity and did act through inhibition of ATP synthase. Supported by Complex II, ADP-stimulated respiration was decreased in the presence of 8-Br-cAMP and again, was not changed by cytochome C or FCCP (Figure 1C).

Altogether, these data demonstrate that endogenous TCA cycle flux alone is insufficient to increase steady-state cAMP levels in isolated skeletal muscle mitochondria and that increased mitochondrial cAMP levels do not increase O_2 flux when measured exclusively through Complex I or II.

The off-target effects of commonly used sAC inhibitors

Previous reports have demonstrated anomalous effects of KH7 suggesting that it may act independent of cAMP/PKA signaling [62, 118]. To determine whether KH7 decreases mitochondrial respiratory capacity via inhibition of cAMP production, GM-supported respiration was measured in isolated liver mitochondria in the absence or presence of 1 mM 8-Br-cAMP to bypass the effects of KH7 of sAC. The presence of 8-Br-cAMP did not alter JO_2 prior to addition of KH7 and more importantly, did not attenuate the complete ablation of ADP-stimulated JO_2

following the addition of 25 μM KH7 (Supp Figure 1B). Notably, JO2 was not restored by the subsequent addition of cytochrome c or FCCP, suggesting that KH7 somehow disrupted electron flow from Complex I to Complex IV. Subsequently, Complex I activity was measured in fragmented mitochondria isolated from skeletal muscle. The addition of KH7 caused an immediate and completion ablation of Complex I activity that was not recovered by the addition of 8-Br-cAMP (Supp Figure 1C). Generation of dose-response curves for Complex I activity as a function of [KH7] revealed an IC_{50} value of 3.7 μM that is comparable to the reported IC_{50} values of KH7 for sAC previously reported [115, 119].

Besides KH7, the only other known sAC inhibitor with an IC_{50} value for sAC below 10 μM is the estrogen metabolite 2-hydroxyestradiol (2-HE) [120]. However, 2-HE has been reported to be capable of generating superoxide via redox cycling [121]. To determine the magnitude and mechanism(s) responsible for superoxide generation via 2-HE, we employed the Amplex Ultra-Red H_2O_2 detection system. In the absence of biological tissue, 2-HE, but not its metabolite 2-methoxyestradiol (2-ME), spontaneously generates oxidants (Supp Figure 1E). Notably, this production of oxidants is blunted in the presence of catalase (Supp. Figure 1F), suggesting that at least a portion of the oxidants generated is in the form of H_2O_2. Oxidant production measured in real-time was dose-dependent (Supp Figure 1G) and detectable even at 200 nM, a concentration at least 50 fold lower than what has been previously used to inhibit sAC in cells [62, 118]. Of note, detection of H_2O_2 with Amplex Red requires the presence of horseradish peroxidase (HRP). Therefore, to validate these findings further, experiments were performed to determine whether 2-HE generated oxidants in the absence of HRP by using O_2 consumption as a surrogate for oxidant production. In the absence of HRP, 2-HE consumed O_2 in a dose-dependent fashion (Supp. Figure 1H).

Altogether, these data provide direct evidence that the two most popular inhibitors of sAC, KH7 and 2-HE, both display off target effects that likely preclude their use for the assessment of

mitochondrial bioenergetics. In light of these findings, neither of these compounds were used for further experimentation.

Inhibition of PKA dose-dependently decreases Complex I-supported respiration.

Inhibition of PKA has been shown to decrease mitochondrial respiratory capacity [67] while it appears unlikely that exogenously increasing cAMP stimulates respiration based previous reports [62] and our data here (see Figures 1B and C). Therefore, we re-tested the hypothesis that inhibition of PKA will decrease mitochondrial respiratory capacity. To test this hypothesis, the same two protocols shown in Figures 1B and C were repeated with isolated liver mitochondria but experiments were performed in the absence or presence of the popular PKA inhibitor H89 [122]. Consistent with previous work and the prevailing hypothesis, H89 dose-dependently decreased ADP-stimulated, Complex I-supported respiration (Figure 2A). However, surprisingly and contrary to previous reports [67], H89 did not decrease ADP-stimulated, Complex II-supported respiration (Figure 2B).

These data suggest that H89, possibly through inhibition of PKA activity, decreases Complex I, but not Complex II, supported respiratory capacity and therefore provides evidence that Complex I may be a target of the functional inhibition incurred by pharmacological inhibition of PKA.

H89-mediated inhibition of PKA alters flux through Complex I.

To further define the effects of H89-mediated PKA inhibition on mitochondrial bioenergetics in the context of Complex I, permeabilized myofibers (PmFBs) from both oxidative and glycolytic mouse skeletal muscle were used. Briefly, PmFBs are structurally intact preparations that are

used to study skeletal muscle mitochondrial function [46] and better reflect *in vivo* respiratory kinetics than isolated mitochondria [93, 95]. Using PmFBs, the hypothesis that inhibition of PKA decreases electron flow through Complex I was first tested by measuring the kinetics of oxidation of Complex I-supported respiratory substrates (e.g. pyruvate and glutamate). In the presence of H89, pyruvate/malate-supported respiration was decreased across the range of [ADP] tested in both RG and WG (Figure 3A and D), consistent with our findings in isolated liver mitochondria (Figure 2A). Furthermore, the [pyruvate] required to elicit 50% of maximal respiration (defined as the apparent K_m) was decreased (Figure 3C and D), indicating a higher sensitivity of OXPHOS for pyruvate oxidation. Concurrently and in further agreement with our findings in isolated liver mitochondria, the maximal rate of respiration (defined as V_{max}) was also decreased in both RG and WG in the presence of H89 (Figure 3C and D). Further supporting these findings, H89 also decreased K_m and V_{max} for glutamate (Figures 3E-H). Collectively, these data suggest that H89, potentially via inhibition of PKA, decreases maximal capacity for substrate oxidation while forcing a greater amount of substrate oxidation to support a given level of metabolic demand.

To further test the hypothesis that PKA inhibition alters electron flow through Complex I, reverse (succinate) and forward (glutamate/malate/rotenone) electron flow-mediated mOEP were measured. In both RG and WG, reverse electron flow-mediated mOEP were decreased by H89 (Figures 3I and J). Subsequent addition of auranofin revealed that this effect was due to decreased oxidant production, not an alteration in oxidant scavenging capacity (Figures 3I and J). Surprisingly, H89 did not alter forward electron flow-mediated oxidant emission in the presence or absence of auranofin (Figures 3K and L). When combined with our findings in pyruvate and glutamate oxidation, these data demonstrate that H89 decreases maximal

capacity for oxidation of NAD^+-linked substrate, increases substrate oxidation at a given level of metabolic demand and decreases electron flow back into, but not forward through, Complex I.

Inhibition of PKA alters ADP kinetics and respiratory control, but not OXPHOS efficiency.

Thus far, the data provided suggest that H89 creates a bottleneck at Complex I of the ETS, however, evidence also exists suggesting that H89 treatment decreases membrane potential [67], possibly by uncoupling oxidative phosphorylation. To test the possibility that inhibition of PKA acts as a mitochondrial uncoupler, we determined the effect of H89 on ADP and OXPHOS efficiency kinetics with Complex I substrates. Consistent with our findings regarding substrate oxidation (see Figures 3A-H), H89 treatment decreased both K_m and V_{max} for ADP (Figures 4A and B). H89 treatment decreased "leak-dependent" respiration (Figure 4C) but somewhat paradoxically also decreased respiratory control ratio (RCR) (Figure 4D), a commonly reported index of respiratory coupling [49].

Since our data provided evidence for both an increase (decreased RCR, Figure 4D) and a decrease (decreased leak-dependent respiration, Figure 4C) in respiratory coupling, we took a more direct approach to test the hypothesis that H89 uncouples oxidative phosphorylation. To achieve this, we used a recently established method [113] to determine OXPHOS efficiency by simultaneously measuring rates of ATP synthesis and O_2 consumption, then calculating the amount of ATP produced per atom of oxygen consumed (e.g. the ATP/O ratio) in real-time and over a range of ADP concentrations. Consistent with our observed effects on respiratory capacity (Figure 2A and Figure 3), H89 decreased rates of O_2 consumption and ATP synthesis (Figures 4E, F, H and I). However, H89 did not decrease ATP/O ratio overall or at any given

[ADP] tested (Figures 4G and J), suggesting that, at least during ATP synthesis, OXPHOS efficiency was preserved.

Altogether, these data provide direct evidence that despite altered respiratory capacity, pharmacological inhibition of PKA does not impact OXPHOS efficiency as measured by the ATP/O ratio.

Discussion

In recent years, starting with the discovery of soluble adenylyl cyclase [60], a role for cAMP signaling in the mitochondrial matrix has emerged, with independent groups revealing the individual components of the signaling cascade , the existence of mitochondrial cAMP/PKA signaling microenvironments [66, 77, 123], and a wide variety of reversibly phosphorylated mitochondrial proteins [76, 124]. Of these findings, two were addressed further in the current report: TCA cycle-dependent activation of sAC via bicarbonate production and governance of oxidative phosphorylation via PKA, particularly at Complex I. First, to date, no direct demonstration of endogenous TCA cycle-dependent activation of sAC has been reported. Furthermore, a number of findings regarding cAMP/PKA-dependent regulation of oxidative phosphorylation are inconsistent with the principles of mitochondrial bioenergetics established by Nobel laureate Peter Mitchell [125] that are supported by nearly 50 years of research. For example, the notion that increasing mitochondrial cAMP levels increases respiration independent of increased metabolic demand implies that cAMP-dependent signaling is somehow limited in actively phosphorylating mitochondria. Given the paramount role that mitochondria play in the maintenance of energy homeostasis, a tonic governance of O_2 flux that is bioenergetically unfavorable (limits ATP synthesis) seems unlikely. In this report, we provide evidence against TCA cycle-derived bicarbonate production as an independent activator of

mitochondrial cAMP levels. Furthermore, addition of exogenous cAMP failed to increase O_2 flux in isolated mitochondria (Figures 1B and C) while inhibition of PKA impaired mitochondrial bioenergetics in both isolated mitochondria (Figure 2) and PmFBs (Figures 3 and 4). Altogether, these findings indicate that, while our understanding of the underlying molecular events involved remains incomplete, the functional impact of mitochondrial cAMP/PKA signaling does appear to conform to principles of mitochondrial bioenergetics. Furthermore, the data provided support the hypothesis that post-translational modifications to Complex I serve as a mechanism to regulate the sensitivity and capacity of OXPHOS to substrates and metabolic demand, electron leak, but not OXPHOS efficiency.

It was shown over a decade ago that exogenous bicarbonate can increase cAMP levels via activation of sAC [60], a finding that has been independently confirmed by multiple groups [61, 62, 110]. In this report, we provide similar findings (Supplemental Figure 1A), but then provide evidence that endogenous CO_2 production from the TCA cycle is insufficient to increase steady-state cAMP levels (Figure 1A). It is noteworthy that our experiments were performed in the presence of EGTA, thereby chelating Ca^{2+}, an activator of sAC [61, 62] and the absence of phosphodiesterase inhibitors. Whether the absence of Ca^{2+} contributed to the lack of effect of TCA cycle flux remains to be seen since perhaps the combination of increased CO_2 production concomitant with increased mitochondrial Ca^{2+} levels could be sufficient to increase mitochondrial cAMP levels. However, certain phosphodiesterases have also been shown to be Ca^{2+}-dependent [126], so it is unclear what the net result would be of Ca^{2+}. The absence of phosphodiesterase inhibitors was intentional as the goal of the experiment was to determine whether endogenous TCA cycle flux increased cAMP “tone”, not simply an increase in production. Finally, the possible effect(s) of exogenous bicarbonate on acidification of matrix pH as shown previously [62] despite experiments being performed with additional pH buffering (300 mM Tris-HCl in the case of Acin-Perez [67] and the current report) are unknown.

The discovery and subsequent characterization of sAC has been instrumental in our understanding of this alternative pathway of cAMP signaling. Defining the role of sAC in the regulation of mitochondrial bioenergetics has hinged greatly on the use of two particular inhibitors: KH7 [67, 84, 85, 115] and 2-hydroxyestradiol [62, 118, 120]. In this report, direct evidence is provided showing that KH7 inhibits mitochondrial respiratory capacity independent of cAMP/PKA signaling (Supp Figure 1B) and may do so via direct inhibition of Complex I (Supp Figure 1C and D). Notably, the only other commercially available inhibitor of sAC with an IC_{50} below 10 μM is 2-HE, but this compound has been reported to participate in redox cycling in cells and cell lysates [121]. However, in this report, it has been revealed that 2-HE is a spontaneous oxidant generator (Supplemental Figure 1E-H) and thus likely leads to oxidation of mitochondrial proteins and consequently, unexpected effects on mitochondrial biology. Altogether, these data, along with previous studies, indicate that the non-specific effects of KH7 and 2-HE preclude their use in the assessment of mitochondrial bioenergetics and that reports using these compounds in attempt to study the link between cAMP/PKA signaling and mitochondrial function need to be carefully re-evaluated. Fortunately, recent work has elucidated the crystal structure of human sAC during catalysis and activation via bicarbonate [127], findings that will likely be instrumental in furthering our understanding of and ability to pharmacologically target sAC.

In this report, data are provided to suggest that increasing cAMP levels using a membrane-permeable cAMP mimetic fails to increase mitochondrial respiratory capacity (Figures 1B and C). These data contradict a previous report [67] that showed an increase in respiratory capacity with 8-Br-cAMP when supported by Complex I, but not Complex II-supported substrates. These authors went on to attribute the effects of cAMP/PKA signaling, at least in part, to cytochrome c oxidase (COX), an electron transporting enzyme of Complex IV of the ETS. However, these conclusions are paradoxical in that, under the experimental conditions used, succinate oxidation

does not generate CO_2, whereas glutamate/malate does. So, if COX is activated by cAMP that is normally produced via TCA cycle-dependent CO_2 production, then addition of exogenous cAMP should have the greatest effect on succinate-supported respiration since CO_2-dependent cAMP production would not be occurring. However, since the existing data do not support this hypothesis, it appears unlikely that increasing cAMP levels facilitates greater oxidative phosphorylation, at least under the experimental conditions tested. Notably, our data agree with recent work [62] that showed that a different PKA agonist caused a reduction in mitochondrial ATP levels, consistent with our observed decrease in respiratory capacity. Ultimately, the existing data provide evidence against mitochondrial cAMP/PKA signaling being activated by endogenous TCA cycle flux in the absence of co-regulators and that increasing cAMP levels beyond endogenous levels does not enhance maximal respiratory capacity.

Despite evidence against exogenous cAMP enhancing respiration, the possibility that PKA activity regulates mitochondrial bioenergetics remains and is supported by multiple lines of evidence [62, 67, 82, 83]. This possibility seems almost inevitable with reports of seventy-five different mouse liver mitochondrial proteins originally identified in the MitoCarta [108] having PKA consensus phosphorylation sites [76, 124]. In the current report, we begin by demonstrating that the popular PKA inhibitor H89 dose-dependently decreases Complex I, but not Complex II, supported respiration (Figures 2A and B), providing initial evidence that Complex I is a putative target of H89. Importantly, an array of literature spanning almost twenty years exists implicating Complex I as a target of PKA-dependent phosphorylation [68, 70, 77]. Subsequently, H89 was used as a tool to inhibit PKA in PmFBs and found that the panoply of effects elicited by H89 on mitochondrial respiratory kinetics, respiratory capacity, oxidant emission and OXPHOS efficiency converge on Complex I. Increased sensitivity of OXPHOS to both Complex I-supported respiratory substrates (Figures 3A-H) and ADP (Figures 4A and B) combined with decreased maximal capacity indicate that a “bottleneck” is established in the

ETS that limits electron flow, possibly at Complex I. Further experiments demonstrated that H89 inhibits reverse, but not forward, electron flow-mediated oxidant emission through Complex I (Figures 3I-L). These data are particularly important as they give topographical insight into where H89 may be acting within Complex I. Electron leak from Complex I is thought to occur at two sites. First is the flavin (F) site, responsible for NADH reduction and the majority of electron leak in the forward direction [2], but was not affected by H89 (Figure 3 K and L). Second, the quinone (Q) site of Complex I, responsible for quinone reduction and the majority of electron leak in the reverse direction, was decreased by PKA inhibition. Altogether, these data suggest that H89 acts on Complex I, possibly through inhibition of PKA-dependent phosphorylation, between these two electron transfer sites, which is at or near the 18 kDa subunit of Complex I. Further strengthening this possibility, these data demonstrate that although H89 inhibits rates of ATP synthesis and O_2 consumption (Figures 4E, F, H and I), no effect on OXPHOS efficiency (as defined by ATP/O ratio) was observed (Figure 4G and J). This suggests that H89 does not uncouple actively phosphorylating mitochondria, and therefore further implicates cAMP/PKA-dependent phosphorylation of Complex I as a functional regulator of electron flow that acts at or near the Q site of electron transfer in Complex I. It should be noted that H89 is not entirely specific for PKA [128], although the data provided collectively suggest that H89 acts on Complex I at the 18 kDa subunit of Complex I, an established site of PKA-dependent phosphorylation.

Conclusions

The field of mitochondrial bioenergetics has become a focal point for the treatment of a variety of genetic and acquired diseases. Within this broad area of study, mitochondrial cAMP/PKA signaling is now an accepted component of the regulation of mitochondrial physiology. In the current report, we further our understanding of mitochondrial cAMP/PKA signaling by providing evidence that, despite exogenous bicarbonate being capable of increasing cAMP levels,

endogenous TCA cycle flux alone may be insufficient to increase mitochondrial cAMP levels. Furthermore, we demonstrate that increasing mitochondrial cAMP levels using a membrane-permeable cAMP mimetic does not increase respiratory capacity. Finally, we provide a comprehensive assessment of the functional consequences of pharmacological inhibition of PKA on the kinetics, efficiency and oxidant emitting potential of mitochondrial bioenergetics. This assessment indicates that Complex I is a primary component of the regulation of mitochondrial bioenergetics by cAMP/PKA signaling and agrees with existing data implicating Complex I as a prime pharmacological target for the treatment of a variety of mitochondrial pathologies.

Figure 8: TCA-cycle dependent cAMP levels and effect of exogenous cAMP on respiratory capacity in isolated mitochondria. A) cAMP was measured in isolated skeletal muscle mitochondria in the presence of 1 mM ATP, and in the absence (white bars) of respiratory substrates or in the presence of pyruvate/malate (black bars), succinate (dark gray bars) or palmitoylcarnitine/malate (light gray bars). Parallel experiments were performed in the presence of KH7, acetazoamide and/or FCCP. N=4/condition. JO_2 supported with substrates for Complex I (A) or Complex II (B) was measured in isolated liver mitochondria in the absence (white bars) or presence (gray bars) of 1 mM 8-Br-cAMP. N=4/condition. * denotes $p < 0.05$ compared to untreated condition.

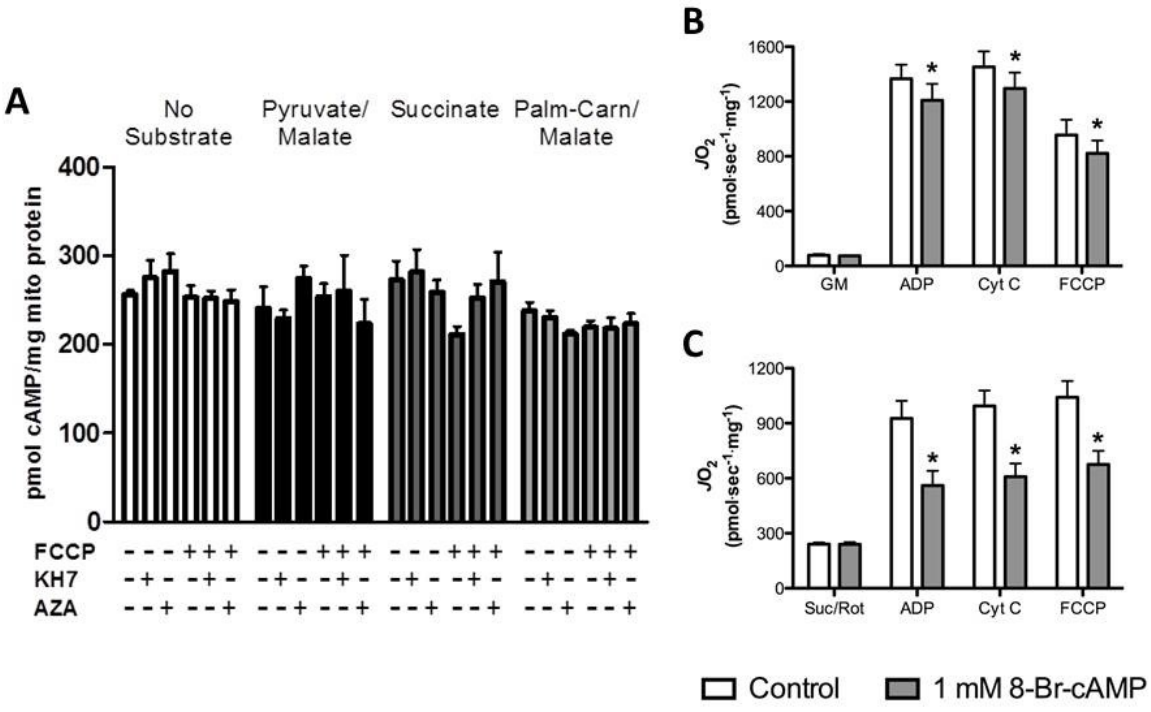
A
No Substrate
Pyruvate/ Malate
Succinate
Palm-Carn/ Malate
pmol cAMP/mg mito protein
400
300
200
100
0
FCCP
KH7
AZA
B
JO_2 (pmol·sec^{-1}·mg^{-1})
1600
1200
800
400
0
GM
ADP
Cyt C
FCCP
C
JO_2 (pmol·sec^{-1}·mg^{-1})
1200
900
600
300
0
Suc/Rot
ADP
Cyt C
FCCP
Control
1 mM 8-Br-cAMP

Supplemental Figure, related to Figure 8. **A**) cAMP was measured in isolated liver mitochondria in the absence or presence of 1 mm ATP, 30 mM $NaCO_3$-and/or 25 μM KH7. **B**) The non-specific effects of KH7 were assessed by measuring Complex I-supported JO_2 measured in the absence (white bars) or presence (gray bars) of 1 mM 8-Br-cAMP to bypass KH7 inhibition of sAC. N=4/condition. **C**) Complex I activity was measured in fragments of isolated skeletal muscle mitochondria following the sequential addition of 25 μM KH7 and 100 μM 8-Br-cAMP. **D**) Dose-response inhibition curve generated for inhibition of Complex I activity as a function of [KH7]. N=3 separate observations. **E**) H2O2 production from 2-methoxyestradiol (2-ME) and 2-hydroxyestradiol (2-HE) was measured using Amplex Ultra Red reagent. N=3 independent observations. **F**) H_2O_2 production by 200 nM 2-HE in the absence (solid line) or presence (dashed line) of 100 U/ml catalase. **G**) Dose-dependent rate of H_2O_2 production of 2-HE over the span of five minutes. N=3 independent experiments. **H**) Dose-dependent O_2 consumption by 2-HE measured in the absence of peroxidases. N=3 independent experiments. * denotes $p<0.05$ compared to DMSO.

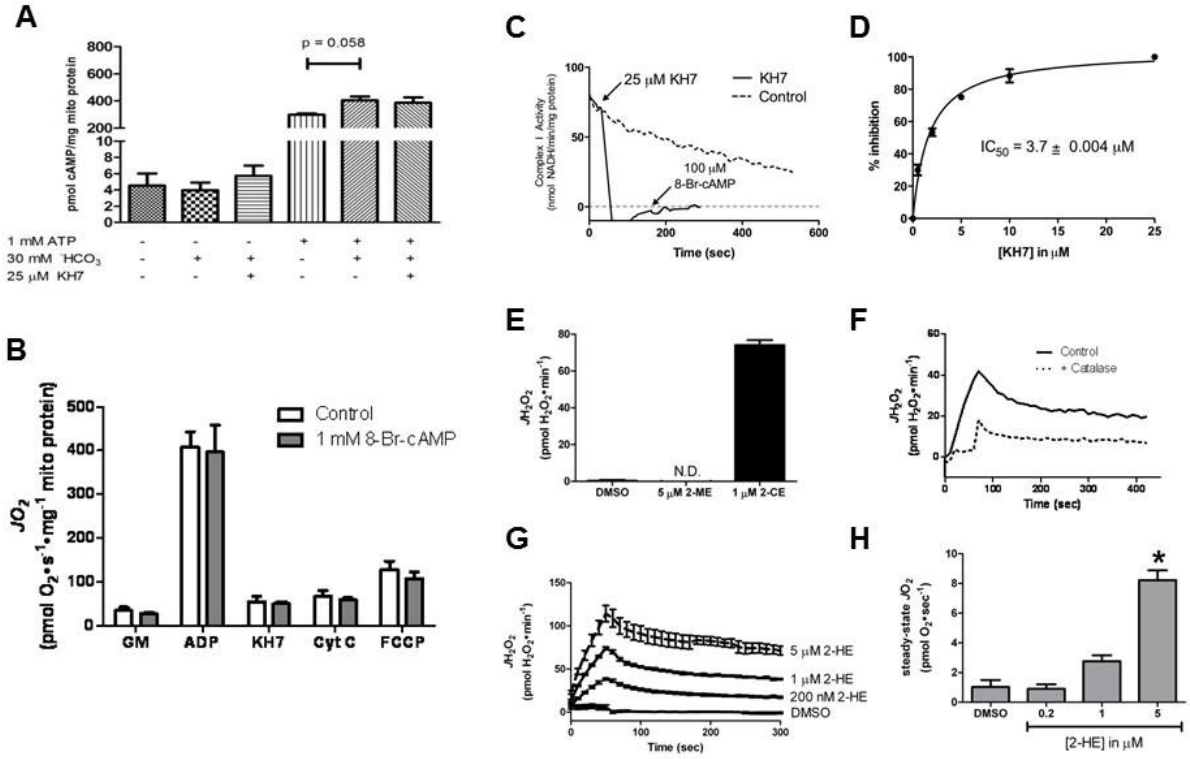
A
p = 0.058
pmol cAMP/mg mito protein
1 mM ATP
30 mM HCO3
25 μM KH7
B
Control
1 mM 8-Br-cAMP
GM
ADP
KH7
Cyt C
FCCP
C
25 μM KH7
KH7
Control
100 μM 8-Br-cAMP
Time (sec)
D
% inhibition
IC50 = 3.7 ± 0.004 μM
[KH7] in μM
E
N.D.
DMSO
5 μM 2-ME
1 μM 2-CE
F
Control
+ Catalase
Time (sec)
G
5 μM 2-HE
1 μM 2-HE
200 nM 2-HE
DMSO
Time (sec)
H
DMSO
[2-HE] in μM

Figure 9: Pharmacological inhibition of PKA dose-dependently decreases Complex I- but not Complex II-supported respiration in isolated liver mitochondria. JO_2 was measured with Complex I (A) or Complex II (B) supported substrates in the absence (white bars) or presence of 1 (black bars), 5 (dark gray bars) or 10 (light gray bars) μM H89. N=4-6/condition. * denotes $P<0.05$ compared to control.

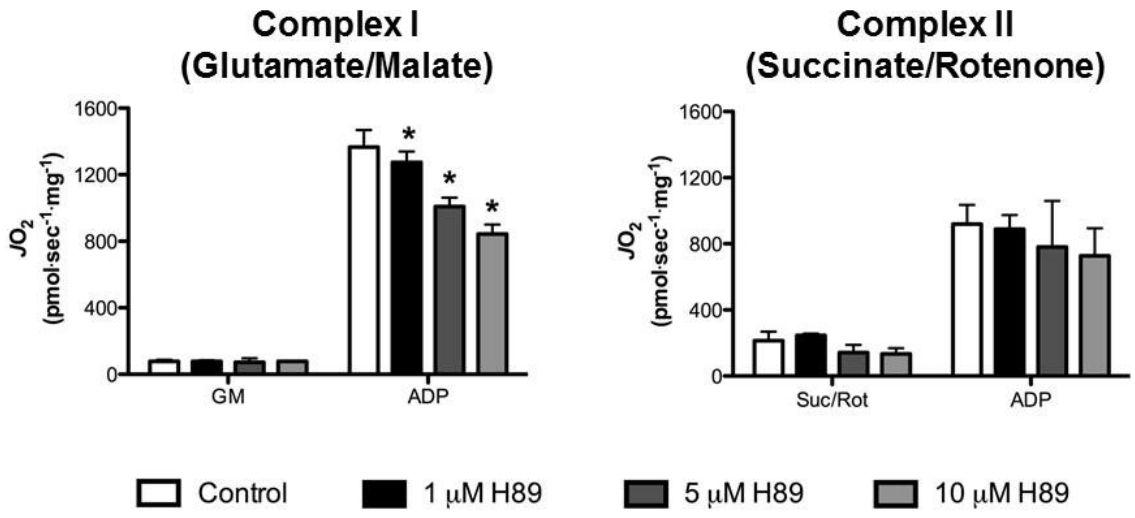
Complex I
(Glutamate/Malate)
Complex II
(Succinate/Rotenone)
JO_2 (pmol·sec^{-1}·mg^{-1})
1600
1200
800
400
0
GM
ADP
Suc/Rot
*
Control
1 μM H89
5 μM H89
10 μM H89

Figure 10: Effects of PKA inhibition on substrate oxidation kinetics and oxidant production in PmFBs. Pyruvate titrations were performed in RG (A) and WG (B) in the absence (circles) or presence (squares) of 10 μM H89. Michaelis-Menten like kinetics analyses for pyruvate in RG (C) and WG (D). N=4-8/condition. * denotes $p<0.05$ compared to Control. Glutamate titrations were performed in RG (E) and WG (F) in the absence (circles) or presence (squares) of 10 μM H89. Michaelis-Menten like kinetic analyses for glutamate in RG (G) and WG (H). N=4-8/condition. * denotes $p<0.05$ compared to Control. H2O2 emission, production and scavenging supported by succinate or glutamate/malate/rotenone were determined in RG (I and K) and WG (J and L) in the absence (white bars) or presence (gray bars) of 10 μM H89. N=4-8/condition. * denotes $p<0.05$ compared to Control.

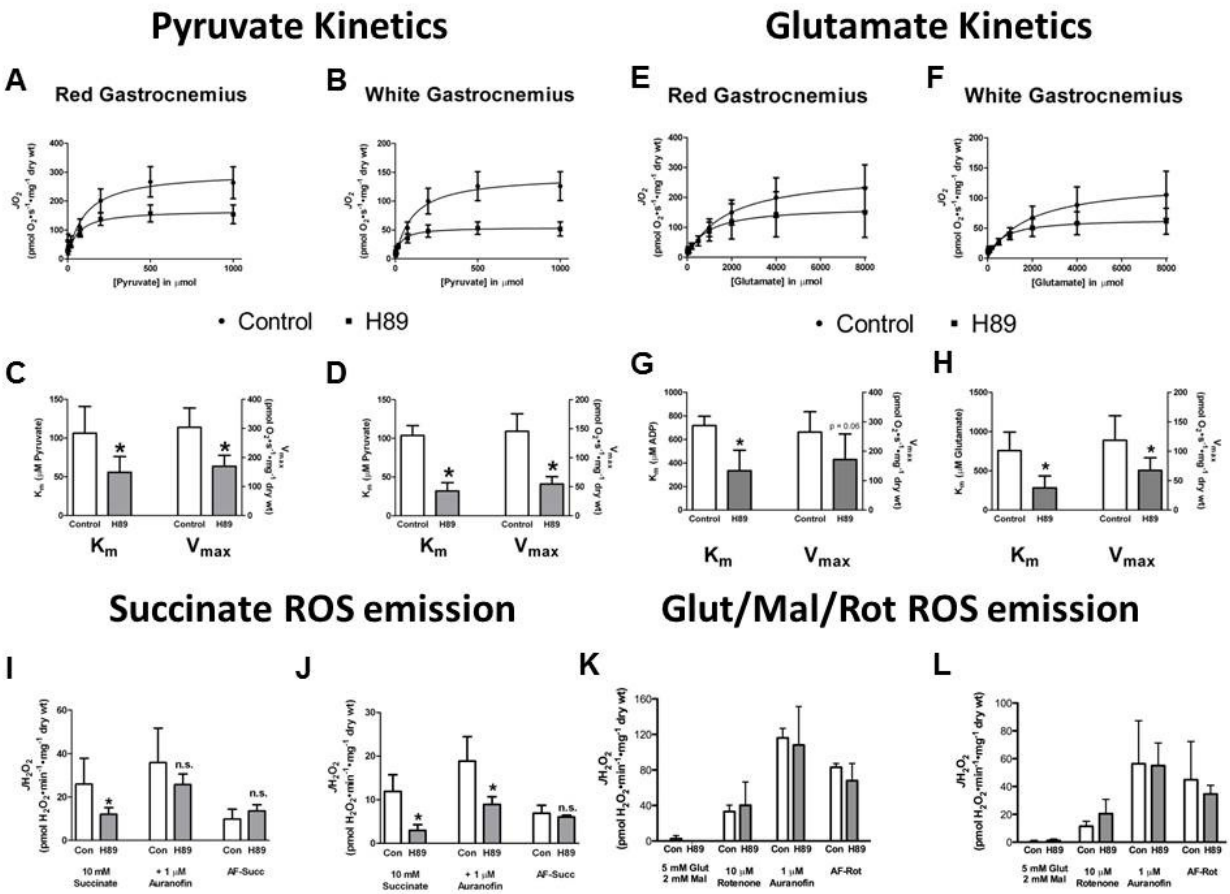
Pyruvate Kinetics
Glutamate Kinetics
A
Red Gastrocnemius
B
White Gastrocnemius
E
Red Gastrocnemius
F
White Gastrocnemius
[Pyruvate] in μmol
[Glutamate] in μmol
• Control ▪ H89
C
D
G
H
Km
Vmax
Control
H89
Succinate ROS emission
Glut/Mal/Rot ROS emission
I
J
K
L
10 mM Succinate
+ 1 μM Auranofin
AF-Succ
5 mM Glut 2 mM Mal
10 μM Rotenone
1 μM Auranofin
AF-Rot
Con
H89
n.s.

Figure 11: Effects of PKA inhibition on ADP kinetics and OXPHOS efficiency in PmFBs. Michaelis-Menten like kinetics were determined from ADP titration experiments in the absence (white bars) or presence (gray bars) of 10 μM H89 in RG (A) and WG (B). C) State 4 JO_2 in the absence (white bars) or presence (gray bars) in RG (left) and WG (right). D) Respiratory control ratio (S3/S4) was determined from ADP titration experiments in the absence (white bars) or presence (gray bars) of 10 μM H89 in RG (left) and WG (right). *J*ATP was determined as a function of [ADP] in the absence (white bars) or presence (gray bars) of 10 μM H89 in RG (E) and WG (F). JO_2 was determined as a function of [ADP] in the absence (white bars) or presence (gray bars) of 10 μM H89 in RG (G) and WG (H). ATP/O ratio was determined as a function of [ADP] in the absence (white bars) or presence (gray bars) of 10 μM H89 in RG (I) and WG (J). N=4-6/condition. * denotes $p<0.05$ compared to Control.

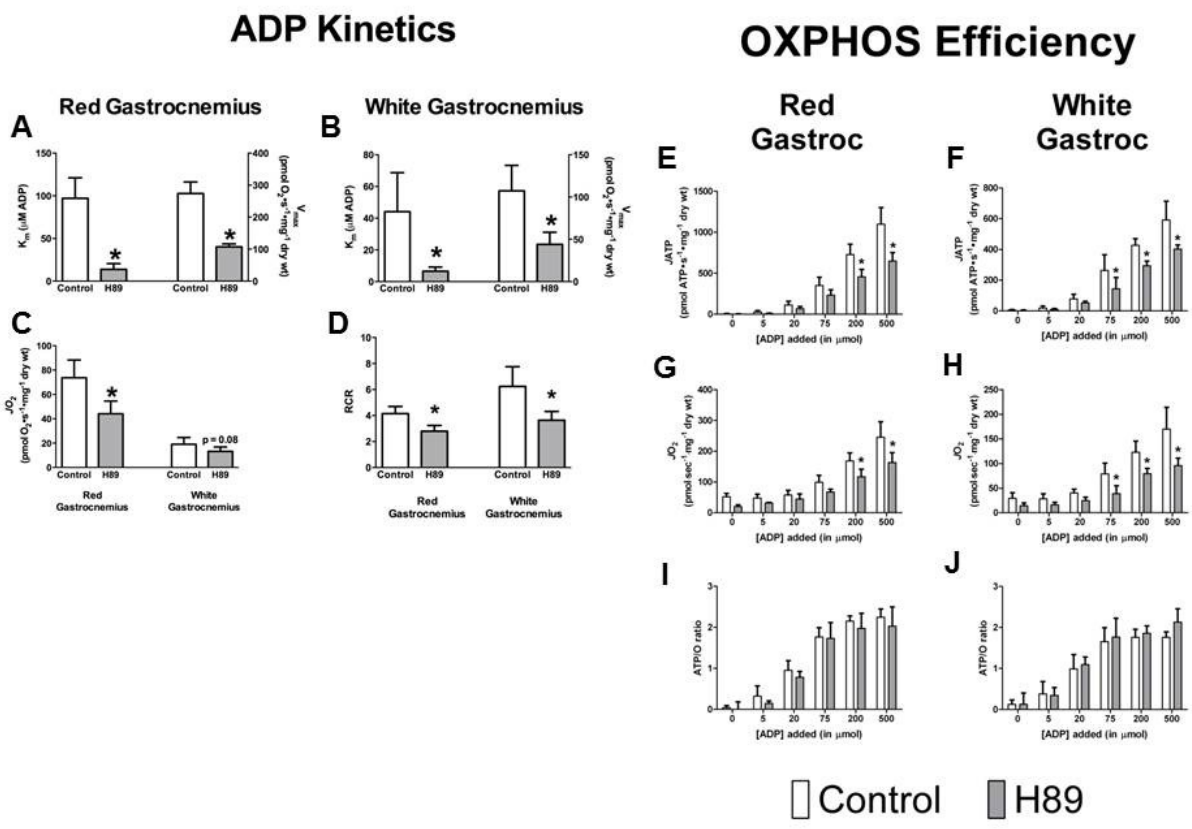
ADP Kinetics
OXPHOS Efficiency
Red Gastrocnemius
White Gastrocnemius
A
B
C
D
E
F
G
H
I
J
Red Gastroc
White Gastroc
Control
H89
p = 0.08
[ADP] added (in μmol)
Red Gastrocnemius
White Gastrocnemius

CHAPTER 4: INTEGRATED DISCUSSION

The mitochondrion is an essential organelle for metabolism in almost every cell type of the human body; as such, understanding its machinery and regulation is integral to effective targeting of mitochondrial function to treat metabolic diseases. In Chapter 1, the existing literature emphasized the need to better understand how OXPHOS efficiency is regulated and to define the functional consequences of phosphorylation of ETS proteins. In Chapter 2, a method was developed to determine OXPHOS efficiency in PmFBs. Using this technique, it was demonstrated that mitochondria respond to metabolic demand by increasing OXPHOS efficiency, illustrating a novel mechanism by which mitochondria can increase ATP production independent of increased O_2 flux. In Chapter 3, it was found that mitochondrial cAMP/PKA signaling was not regulated by TCA cycle flux, but that PKA activity governs electron flow through Complex I of the ETS. Together, the data reported here provide a notable advance in the scientific literature by revealing the kinetic nature of OXPHOS efficiency and demonstrating that phosphorylation of Complex I is an important regulator of mitochondrial physiology.

In Chapters 2 and 3, PmFBs were used to assess mitochondrial bioenergetics while isolated mitochondria were also used in Chapter 3. Both isolated mitochondria and PmFBs have limitations that need to be taken into account when interpreting findings. For example, O_2 flux in PmFBs has been suggested to be limited by O_2 diffusion into the core of the bundle [129]. However, inhibition of contraction, as was achieved in these studies by the addition of blebbistatin, mitigates this issue [93]. Additionally, PmFBs retain many structural elements that are eliminated in isolated mitochondria [95], so the possibility for extramitochondrial regulation is possible, like that incurred by tubulin [130]. Of note, the effects of tubulin on PmFB function appear to be physiologically relevant and not artifact of the preparation [130, 131]. In isolated mitochondria, limitations are mostly based on the differential centrifugation procedure since it has been shown to damage mitochondria [95] and even omit populations, such that it is thought

that “healthy” mitochondria are selectively obtained from samples [95, 132]. Conversely, PmFBs are treated with a mild detergent but not subjected to shear stress like isolated mitochondria [132], therefore, it is thought that all mitochondria in a given sample are retained. Perhaps the most relevant comparison to the current reports, the kinetic response of isolated mitochondria compared to PmFBs to [ADP] is strikingly different. For example, in both myocardium and skeletal muscle, the K_m for ADP in isolated mitochondria is orders of magnitude lower, implying greater sensitivity, than in PmFBs [90, 133]. Importantly, resting [ADP] in skeletal muscle is estimated to be < 20 μM [103, 104], while the K_m for ADP in isolated mitochondria is typically reported as ~20 μM. Therefore, using isolated mitochondria, it would be deduced that mitochondria at rest operate at ~50% of maximal capacity. Conversely, PmFBs experiments performed in the current report predict that mitochondria operate at ~20% of maximal capacity. Extended even further, performing experiments in the presence of a phosphocreatine (PCr) to creatine (Cr) ratio of 2:1 increases the K_m for ADP to the mM range in human PmFBs, predicting that mitochondria operate at ~1% of maximal capacity at rest *in vivo* [93]. Unfortunately, due to methodological reasons, phosphocreatine could not be added when measuring OXPHOS efficiency as described.

In Chapter 2, the primary finding was that OXPHOS efficiency increased as a function of the amount of ADP added. This observation is consistent with a recent report in isolated rat skeletal muscle mitochondria [57] using a similar technique and measurements in permeabilized human atrium using the technique described here [113], altogether suggesting that demand-driven enhancement of OXPHOS efficiency may be a conserved bioenergetic response across all eukaryotic species. If confirmed, this would be of profound importance, since muscular work *in vivo* is thought to be in large part limited by O_2 diffusion into tissues [134, 135]. Therefore, demand-driven enhancement of OXPHOS efficiency would represent a fundamental

physiological mechanism allowing mitochondria to maximize ATP production at a given rate of O_2 flux and have relevance in every mitochondrion-containing tissue.

An example of the potential significance of demand-driven enhancement of OXPHOS efficiency would be in cancer cell biology. Cancer cells are characterized by a metabolic shift towards anaerobic glucose metabolism to support their growth and proliferation, termed the Warburg effect. It is thought that this increased reliance on anaerobic metabolism is in part due to limited O_2 diffusion into the tumor [136]. However, despite this increased reliance on glucose as a metabolic substrate, disruption of OXPHOS impairs cancer cell growth and proliferation [137, 138]. Considered in the context of the data provided in Chapter 2, it is possible that impairing the ability of mitochondria to maintain a high OXPHOS efficiency in tumor cells during proliferation could be a powerful strategy to blunt tumor growth. Also, in contrast to most other chemotherapeutic approaches, preventing the enhancement of OXPHOS efficiency as opposed to attempting to directly kill cancer cells reduce the death of non-cancerous cells. Supporting this hypothesis, the mitochondrial uncoupler FCCP has been shown to attenuate lung cancer cell growth [139]. Unfortunately, the effective therapeutic dosing window for FCCP (and other uncouplers like 2-dinitrophenol) is rather narrow, so alternative uncouplers with a wider dynamic range would likely be of greater clinical utility [140].

Demand-driven enhancement of OXPHOS efficiency, as described in Chapter 2, appears to be a logical adaptation in a biological system responsible for both managing energy supply and supporting metabolic demand; however, the regulation of OXPHOS is complex. So, although improved OXPHOS efficiency could be due to decreased proton conductance, the possibility that metabolic demand alters the conductance of other cations cannot be ruled out. For example, Ca^{2+} uptake from the mitochondria is an important component of cellular homeostasis, particularly in striated muscle [141]. It has been established that ER-mitochondria Ca^{2+} cross-talk occurs [142], so although the experiments performed here were performed in the presence

of EGTA, this does not preclude the possibility that mitochondrial Ca^{2+} fluxes to and from the endoplasmic reticulum (ER) could be occurring independent of EGTA-mediated Ca^{2+} chelation. Other potential cations that could contribute to mitochondrial energetics and the regulation of OXPHOS efficiency are Mg^{2+} (used at 5 mM in all experiments described), a cofactor for ATPase reactions, Mn^{2+}(not added for the experiments described herein), a co-factor for enzymatic scavenging of superoxide and Na^{+}. Mitochondrial Na^{+}/Ca^{2+} exchange was first reported forty years ago [143], but only recently has the molecular basis for its occurrence been defined as the NCX protein [144]. Through NCX, the actions of Ca^{2+} as described above could also occur, again through the ER-mitochondrial coupling. Ultimately, further experimentation, particularly by utilizing pharmacological and genetic tools to alter cation flux (e.g. manipulating MCU and/or NCX activity or content) and measuring membrane potential, will be crucial in deciphering the mechanism(s) responsible for demand-driven enhancement of OXPHOS efficiency as described here.

In Chapter 3, evidence is provided that suggests that mitochondrial cAMP/PKA signaling governs mitochondrial bioenergetics, but not via changes in TCA cycle flux. A number of important factors need to be considered when evaluating the effects of TCA cycle flux on mitochondrial cAMP levels measured in the current report. First, experiments were not performed in the presence of PDE inhibitors; therefore, the cAMP levels measured were not purely production, but a balance of cAMP production and degradation as they are found *in vivo*. However, due to the omission of PDE inhibitors, it is possible that the window of time when cAMP levels were transiently elevated was missed, resulting in a false negative determination. However, experiments were specifically designed to avoid this possibility by using saturating concentrations of substrates such that “steady-state” conditions were established, if possible. Second, experiments were performed in the absence of Ca^{2+}, a known co-activator of sAC [61]. However, Litvin et al. demonstrated that Ca^{2+} governs the kinetics of sAC activity, but that ATP

determines V_{max}. Therefore, it is not anticipated that the absence of PDE inhibitors or Ca^{2+} would limit the ability to detect changes in sAC-mediated cAMP production, although further experimentation is warranted to directly test these possibilities.

The main finding in Chapter 3 was that pharmacological inhibition of PKA impairs mitochondrial bioenergetics in a way that converges on Complex I of the ETS. However, a notable caveat to the findings presented here is that although these experiments used mitochondrial preparations and were designed to determine the role of PKA activity on mitochondrial bioenergetics, the potential contribution of extramitochondrial PKA should be considered. In striated muscle, the cross-bridge cycling that occurs following Ca^{2+} release and the sequestration of Ca^{2+} by the ER require large amounts of ATP, therein necessitating increased mitochondrial ATP production. Indeed, the data provided here support this generalized role of PKA, as inhibition of PKA activity decreases mitochondrial respiratory capacity, which would limit the ability of mitochondria to support the increased energy expenditure characteristic of G-protein coupled activation of PKA. Intriguingly, the administration of clenbuterol, an agonist of the β2 adrenergic receptor, stimulates thermogenesis [145], suggesting an uncoupling of OXPHOS. Furthermore, administration of clenbuterol decreases skeletal muscle mitochondrial content [146], expression of oxidative enzymes [147, 148] and elicits changes in mitochondrial ultrastructure [149], but to the author's knowledge, no studies have directly examined the role of β2-agonists on mitochondrial respiratory coupling in skeletal muscle. Altogether, the effects of clenbuterol appear to be pursuant with observed effects of increasing cAMP levels using 8-Br-cAMP in the current project, where a decrease, instead of an increase, in JO_2 was observed.

Complex I is a multi-subunit complex that oxidizes NADH on the matrix side of the inner membrane, then transfers electrons to ubiquinone within the inner membrane. Between these two sites of electron transfer lies the 18 kDa accessory subunit of Complex I [150]. Discussed in Chapter 1, a preponderance of evidence indicates that PKA-dependent phosphorylation of

the 18 kDa subunit of Complex I regulates its assembly and function. However, up to 75 different mitochondrial proteins are potential targets of PKA-dependent phosphorylation, so it was unknown whether the effect(s) of pharmacological inhibition of PKA on OXPHOS were due to changes in Complex I function. Using a comprehensive, multi-faceted, kinetics-based assessment of mitochondrial bioenergetics, it was demonstrated that H89, an established PKA inhibitor [122], impairs both the kinetics and capacity of OXPHOS by impairing electron flow through Complex I between the two established sites of electron flow within Complex I. A critical caveat to the evaluation of this data is that H89 has been shown to inhibit a variety of other protein kinases [128], including Rho- and Ca^{2+}/calmodulin-activated protein kinase (CaMK). Rho-kinase is primarily involved in regulating cell shape and structure by acting on the actin cytoskeleton [151]. Importantly, although no studies to our knowledge have sought to determine whether it is located within mitochondria, Rho-kinase has been shown to regulate mitochondrial apoptosis [152]. By contrast, as its name implies, CaMK is activated by Ca^{2+}, which is readily taken up by mitochondria [153]. CaMK has been shown to govern mitochondrial fission via dynamin-related protein 1 (DRP1) [154] although, to our knowledge, no studies to date have addressed the possibility of CaMK being present within mitochondria. Accordingly, it is unlikely that H89-induced inhibition of CaMK in the cytosol is relevant in the current report because experiments were performed in the presence of 1 mM EGTA, a Ca^{2+}-chelating agent. Altogether, the non-specific effects of H89 present the possibility that the effects observed may not be exclusively regulated by PKA. However, the possibility that H89 acts on Complex I at or near the 18 kDa subunit of Complex I remains intact. Future studies could include the use of targeted genetic approaches to mutate phosphorylation sites within Complex I to determine their ultimate effect on mitochondrial function.

In Chapter 2, skeletal muscle OXPHOS efficiency at resting [ADP] (20 μM) was ~20% of the calculated mechanistic ATP/O ratio, so under these conditions, a majority of O_2 flux is attributed

to proton leak. Conversely, in the presence of demand (>75 μM ADP), OXPHOS efficiency is ~70%, meaning that the majority of O_2 flux contributes to supporting ATP synthesis. This >3 fold increase in OXPHOS efficiency reflects a profound alteration in how substrate oxidation contributes to cellular physiology. Furthermore, the kinetics of OXPHOS efficiency (e.g. the relationship between OXPHOS efficiency and [ADP]) may be a measurable determinant of elite athletic performance. Take, for example, two athletes competing in an endurance event (e.g. a marathon). If these two individuals were identical in all other aspects, including mitochondrial content and maximal OXPHOS efficiency, the individual with the more sensitive OXPHOS efficiency response to metabolic demand could have a bioenergetic advantage. Specifically, this individual may be capable of producing more ATP at a given level of O_2 flux, allowing them to perform more work at the same rate of substrate oxidation, or more importantly, to perform the same amount of work while oxidizing less substrate. Oxidation of glucose is an important determinant of marathon running performance because the proverbial "wall" is hit when muscle glycogen stores are essentially depleted. Therefore, the ability to perform the same amount of work at a lower rate of glucose oxidation would be a measurable (and possibly trainable) advantage for an endurance athlete, and in this way, OXPHOS efficiency kinetics may be part of what makes an athlete "elite".

In addition to the implications for sport performance, OXPHOS efficiency could be a meaningful indicator of clinical exercise tolerance. Given the established ACSM guidelines for physical activity and the challenges inherent to the prescription of exercise in at-risk populations, it is crucial that we understand why individuals differ both in their tolerance of prescribed exercise and their willingness to participate in exercise programs. While future studies are needed to first test the relevance of demand-driven OXPHOS efficiency in the context of exercise performance, measuring OXPHOS efficiency in at-risk populations may ultimately provide physiological insights that will improve clinical exercise prescription.

The potential relationship between OXPHOS efficiency and metabolic disease is complex and requires consideration of ATP/O ratio both at rest and in the presence of metabolic demand. First, since OXPHOS efficiency is inversely related to proton leak, which is known to dissipate oxidant production from ETS complexes, it could be reasonably hypothesized that greater OXPHOS efficiency at rest would lead to a greater susceptibility to insulin resistance following high fat feeding. However, it is anticipated that athletes will display a high level of OXPHOS efficiency in the presence of metabolic demand. This paradox is similar to the "athlete's paradox" where intramuscular triglyceride levels are elevated in athletes despite a high degree of insulin sensitivity in that metabolic demand is the differentiating feature between insulin sensitive and insulin resistant individuals despite similar phenotypes.

Conclusions

In summary, the Chapters described here highlight the dynamic nature of mitochondria in two ways: 1) mitochondria respond to metabolic demand by increasing OXPHOS efficiency and 2) PKA-dependent phosphorylation governs respiratory kinetics and capacity. Given the vast number of diseases causally linked to altered mitochondrial metabolism, the development of novel approaches to assess mitochondrial physiology will improve our ability to define and then treat defects in mitochondrial function. In Chapter 2, such an approach is provided where OXPHOS efficiency can be determined as a function of metabolic demand in PmFBs. In addition to the potential diagnostic applications of this technique, it was discovered that mitochondria are capable of increasing ATP production without increasing O_2 flux by increasing OXPHOS efficiency. Defining the mechanism(s) responsible for enhanced OXPHOS efficiency will likely yield advances in the development of novel drug targets to treat metabolic disease. In Chapter 3, the role of mitochondrial cAMP/PKA signaling in the context of mitochondrial bioenergetics was assessed. In the current document, it was demonstrated that pharmacological inhibition of PKA in PmFBs impaired mitochondrial respiratory kinetics,

capacity, oxidant production and ATP synthesis, but not OXPHOS efficiency. Altogether, the data provided suggest that Complex I is a target of PKA-dependent phosphorylation, findings that are corroborated by a number of previous reports. Ultimately, although mitochondrial bioenergetics are regulated in a complex and dynamic fashion, the studies described herein answer important questions and provide tools that are desperately needed to further enhance our understanding of this essential organelle.

REFERENCES

1. Jones, D.P., *Radical-free biology of oxidative stress.* Am J Physiol Cell Physiol, 2008. **295**(4): p. C849-68.
2. Treberg, J.R., C.L. Quinlan, and M.D. Brand, *Evidence for two sites of superoxide production by mitochondrial NADH-ubiquinone oxidoreductase (complex I).* J Biol Chem, 2011. **286**(31): p. 27103-10.
3. Fisher-Wellman, K.H., et al., *Mitochondrial glutathione depletion reveals a novel role for the pyruvate dehydrogenase complex as a key HO-emitting source under conditions of nutrient overload.* Free Radic Biol Med, 2013. **65C**(19): p. 1201-1208.
4. Hu, J., L. Dong, and C.E. Outten, *The Redox Environment in the Mitochondrial Intermembrane Space Is Maintained Separately from the Cytosol and Matrix.* Journal of Biological Chemistry, 2008. **283**(43): p. 29126-29134.
5. Kemp, M., Y.M. Go, and D.P. Jones, *Nonequilibrium thermodynamics of thiol/disulfide redox systems: a perspective on redox systems biology.* Free Radic Biol Med, 2008. **44**(6): p. 921-37.
6. Anderson, E.J., et al., *Mitochondrial H2O2 emission and cellular redox state link excess fat intake to insulin resistance in both rodents and humans.* The Journal of Clinical Investigation, 2009. **119**(3): p. 573-581.
7. Kane, D.A., et al., *Metformin selectively attenuates mitochondrial H2O2 emission without affecting respiratory capacity in skeletal muscle of obese rats.* Free Radic Biol Med, 2010. **49**(6): p. 1082-7.
8. Kloner, R.A., et al., *Reduction of ischemia/reperfusion injury with bendavia, a mitochondria-targeting cytoprotective Peptide.* J Am Heart Assoc, 2012. **1**(3): p. e001644.

9. Houstis, N., E.D. Rosen, and E.S. Lander, *Reactive oxygen species have a causal role in multiple forms of insulin resistance.* Nature, 2006. **440**(7086): p. 944-8.
10. Hatefi, Y. and M. Yamaguchi, *Nicotinamide nucleotide transhydrogenase: a model for utilization of substrate binding energy for proton translocation.* FASEB J, 1996. **10**(4): p. 444-52.
11. Lambert, A.J. and M.D. Brand, *Superoxide production by NADH:ubiquinone oxidoreductase (complex I) depends on the pH gradient across the mitochondrial inner membrane.* Biochem J, 2004. **382**(Pt 2): p. 511-7.
12. Ghezzi, P., *Regulation of protein function by glutathionylation.* Free Radic Res, 2005. **39**(6): p. 573-80.
13. Mieyal, J.J., et al., *Molecular mechanisms and clinical implications of reversible protein S-glutathionylation.* Antioxid Redox Signal, 2008. **10**(11): p. 1941-88.
14. Hurd, T.R., et al., *Glutathionylation of mitochondrial proteins.* Antioxid Redox Signal, 2005. **7**(7-8): p. 999-1010.
15. Beer, S.M., et al., *Glutaredoxin 2 catalyzes the reversible oxidation and glutathionylation of mitochondrial membrane thiol proteins: implications for mitochondrial redox regulation and antioxidant DEFENSE.* J Biol Chem, 2004. **279**(46): p. 47939-51.
16. Mailloux, R.J., et al., *Glutaredoxin-2 is Required to Control Oxidative Phosphorylation in Cardiac Muscle by Mediating Deglutathionylation Reactions.* J Biol Chem, 2014. **2014**: p. 12.
17. Mailloux, R.J., et al., *Glutaredoxin-2 is required to control proton leak through uncoupling protein-3.* J Biol Chem, 2013. **288**(12): p. 8365-79.
18. Mailloux, R.J., S.L. McBride, and M.E. Harper, *Unearthing the secrets of mitochondrial ROS and glutathione in bioenergetics.* Trends Biochem Sci, 2013. **38**(12): p. 592-602.
19. Rolfe, D.F. and M.D. Brand, *Contribution of mitochondrial proton leak to skeletal muscle respiration and to standard metabolic rate.* Am J Physiol, 1996. **271**(4 Pt 1): p. C1380-9.

20. Harper, J.A., K. Dickinson, and M.D. Brand, *Mitochondrial uncoupling as a target for drug development for the treatment of obesity.* Obes Rev, 2001. **2**(4): p. 255-65.

21. Divakaruni, A.S. and M.D. Brand, *The regulation and physiology of mitochondrial proton leak.* Physiology (Bethesda), 2011. **26**(3): p. 192-205.

22. Azzu, V. and M.D. Brand, *The on-off switches of the mitochondrial uncoupling proteins.* Trends Biochem Sci, 2010. **35**(5): p. 298-307.

23. Nicholls, D.G., V.S. Bernson, and G.M. Heaton, *The identification of the component in the inner membrane of brown adipose tissue mitochondria responsible for regulating energy dissipation.* Experientia Suppl, 1978. **32**: p. 89-93.

24. Azzu, V., et al., *Dynamic regulation of uncoupling protein 2 content in INS-1E insulinoma cells.* Biochim Biophys Acta, 2008. **1777**(10): p. 1378-83.

25. Fleury, C., et al., *Uncoupling protein-2: a novel gene linked to obesity and hyperinsulinemia.* Nat Genet, 1997. **15**(3): p. 269-72.

26. Pecqueur, C., et al., *Uncoupling protein 2, in vivo distribution, induction upon oxidative stress, and evidence for translational regulation.* J Biol Chem, 2001. **276**(12): p. 8705-12.

27. Bezaire, V., et al., *Constitutive UCP3 overexpression at physiological levels increases mouse skeletal muscle capacity for fatty acid transport and oxidation.* FASEB J, 2005. **19**(8): p. 977-9.

28. Nabben, M., et al., *The effect of UCP3 overexpression on mitochondrial ROS production in skeletal muscle of young versus aged mice.* FEBS Lett, 2008. **582**(30): p. 4147-52.

29. MacLellan, J.D., et al., *Physiological increases in uncoupling protein 3 augment fatty acid oxidation and decrease reactive oxygen species production without uncoupling respiration in muscle cells.* Diabetes, 2005. **54**(8): p. 2343-50.

30. Lombardi, A., et al., *UCP3 translocates lipid hydroperoxide and mediates lipid hydroperoxide-dependent mitochondrial uncoupling.* J Biol Chem, 2010. **285**(22): p. 16599-605.

31. Anderson, E.J., H. Yamazaki, and P.D. Neufer, *Induction of Endogenous Uncoupling Protein 3 Suppresses Mitochondrial Oxidant Emission during Fatty Acid-supported Respiration.* Journal of Biological Chemistry, 2007. **282**(43): p. 31257-31266.

32. Toime, L.J. and M.D. Brand, *Uncoupling protein-3 lowers reactive oxygen species production in isolated mitochondria.* Free Radic Biol Med, 2010. **49**(4): p. 606-11.

33. Choi, C.S., et al., *Overexpression of uncoupling protein 3 in skeletal muscle protects against fat-induced insulin resistance.* J Clin Invest, 2007. **117**(7): p. 1995-2003.

34. Cadenas, S., et al., *The basal proton conductance of skeletal muscle mitochondria from transgenic mice overexpressing or lacking uncoupling protein-3.* J Biol Chem, 2002. **277**(4): p. 2773-8.

35. Harper, M.E., et al., *Decreased mitochondrial proton leak and reduced expression of uncoupling protein 3 in skeletal muscle of obese diet-resistant women.* Diabetes, 2002. **51**(8): p. 2459-66.

36. Tiraby, C., et al., *Resistance to high-fat-diet-induced obesity and sexual dimorphism in the metabolic responses of transgenic mice with moderate uncoupling protein 3 overexpression in glycolytic skeletal muscles.* Diabetologia, 2007. **50**(10): p. 2190-9.

37. Bevilacqua, L., et al., *Absence of uncoupling protein-3 leads to greater activation of an adenine nucleotide translocase-mediated proton conductance in skeletal muscle mitochondria from calorie restricted mice.* Biochim Biophys Acta, 2010. **1797**(8): p. 1389-97.

38. Nabben, M., et al., *Significance of uncoupling protein 3 in mitochondrial function upon mid- and long-term dietary high-fat exposure.* FEBS Lett, 2011. **585**(24): p. 4010-7.

39. Nabben, M., et al., *Uncoupled respiration, ROS production, acute lipotoxicity and oxidative damage in isolated skeletal muscle mitochondria from UCP3-ablated mice.* Biochim Biophys Acta, 2011. **1807**(9): p. 1095-105.

40. Brand, M.D., et al., *The basal proton conductance of mitochondria depends on adenine nucleotide translocase content.* Biochem J, 2005. **392**(Pt 2): p. 353-62.

41. Echtay, K.S., et al., *A signalling role for 4-hydroxy-2-nonenal in regulation of mitochondrial uncoupling.* EMBO J, 2003. **22**(16): p. 4103-10.

42. Cadenas, S., et al., *AMP decreases the efficiency of skeletal-muscle mitochondria.* Biochem J, 2000. **351 Pt 2**: p. 307-11.

43. Skulachev, V.P., *Uncoupling: new approaches to an old problem of bioenergetics.* Biochim Biophys Acta, 1998. **1363**(2): p. 100-24.

44. Chance, B. and G.R. Williams, *Respiratory enzymes in oxidative phosphorylation. I. Kinetics of oxygen utilization.* J Biol Chem, 1955. **217**(1): p. 383-93.

45. Hinkle, P.C., *P/O ratios of mitochondrial oxidative phosphorylation.* Biochim Biophys Acta, 2005. **1706**(1-2): p. 1-11.

46. Kuznetsov, A.V., et al., *Analysis of mitochondrial function in situ in permeabilized muscle fibers, tissues and cells.* Nat Protoc, 2008. **3**(6): p. 965-76.

47. Perry, C.G., et al., *Methods for assessing mitochondrial function in diabetes.* Diabetes, 2013. **62**(4): p. 1041-53.

48. Nicholls, D.G. and S.J. Ferguson, *Bioenergetics 4.* Amsterdam ; Boston: Academic Press, 2013.

49. Brand, M.D. and D.G. Nicholls, *Assessing mitochondrial dysfunction in cells.* Biochem J, 2011. **435**(2): p. 297-312.

50. Perry, C.G., et al., *High-intensity aerobic interval training increases fat and carbohydrate metabolic capacities in human skeletal muscle.* Appl Physiol Nutr Metab, 2008. **33**(6): p. 1112-23.

51. Galkin, A.S., V.G. Grivennikova, and A.D. Vinogradov, *-->H+/2e- stoichiometry in NADH-quinone reductase reactions catalyzed by bovine heart submitochondrial particles.* FEBS Lett, 1999. **451**(2): p. 157-61.

52. Trumpower, B.L., *The protonmotive Q cycle. Energy transduction by coupling of proton translocation to electron transfer by the cytochrome bc1 complex.* J Biol Chem, 1990. **265**(20): p. 11409-12.

53. Antonini, G., et al., *Proton pumping by cytochrome oxidase as studied by time-resolved stopped-flow spectrophotometry.* Proc Natl Acad Sci U S A, 1993. **90**(13): p. 5949-53.

54. Stock, D., A.G. Leslie, and J.E. Walker, *Molecular architecture of the rotary motor in ATP synthase.* Science, 1999. **286**(5445): p. 1700-5.

55. Watt, I.N., et al., *Bioenergetic cost of making an adenosine triphosphate molecule in animal mitochondria.* Proc Natl Acad Sci U S A, 2010. **107**(39): p. 16823-7.

56. Cross, R.J., J.V. Taggart, and et al., *Studies on the cyclophorase system; the coupling of oxidation and phosphorylation.* J Biol Chem, 1949. **177**(2): p. 655-78.

57. Gouspillou, G., et al., *Accurate determination of the oxidative phosphorylation affinity for ADP in isolated mitochondria.* PLoS One, 2011. **6**(6): p. e20709.

58. Gouspillou, G., et al., *Mitochondrial energetics is impaired in vivo in aged skeletal muscle.* Aging Cell, 2014. **13**(1): p. 39-48.

59. Rall, T.W. and E.W. Sutherland, *Formation of a cyclic adenine ribonucleotide by tissue particles.* J Biol Chem, 1958. **232**(2): p. 1065-76.

60. Buck, J., et al., *Cytosolic adenylyl cyclase defines a unique signaling molecule in mammals.* Proc Natl Acad Sci U S A, 1999. **96**(1): p. 79-84.

61. Litvin, T.N., et al., *Kinetic properties of "soluble" adenylyl cyclase. Synergism between calcium and bicarbonate.* J Biol Chem, 2003. **278**(18): p. 15922-6.

62. Di Benedetto, G., et al., *Mitochondrial Ca(2)(+) uptake induces cyclic AMP generation in the matrix and modulates organelle ATP levels.* Cell Metab, 2013. **17**(6): p. 965-75.

63. Jaiswal, B.S. and M. Conti, *Calcium regulation of the soluble adenylyl cyclase expressed in mammalian spermatozoa.* Proc Natl Acad Sci U S A, 2003. **100**(19): p. 10676-81.

64. Chen, Y., et al., *Soluble adenylyl cyclase as an evolutionarily conserved bicarbonate sensor.* Science, 2000. **289**(5479): p. 625-8.

65. Di Benedetto, G., et al., *Protein kinase A type I and type II define distinct intracellular signaling compartments.* Circ Res, 2008. **103**(8): p. 836-44.

66. Acin-Perez, R., et al., *A phosphodiesterase 2A isoform localized to mitochondria regulates respiration.* J Biol Chem, 2011. **286**(35): p. 30423-32.

67. Acin-Perez, R., et al., *Cyclic AMP produced inside mitochondria regulates oxidative phosphorylation.* Cell Metab, 2009. **9**(3): p. 265-76.

68. Sardanelli, A.M., et al., *Characterization of proteins phosphorylated by the cAMP-dependent protein kinase of bovine heart mitochondria.* FEBS Lett, 1995. **377**(3): p. 470-4.

69. Schwoch, G., B. Trinczek, and C. Bode, *Localization of catalytic and regulatory subunits of cyclic AMP-dependent protein kinases in mitochondria from various rat tissues.* Biochem J, 1990. **270**(1): p. 181-8.

70. Technikova-Dobrova, Z., A.M. Sardanelli, and S. Papa, *Phosphorylation of mitochondrial proteins in bovine heart. Characterization of kinases and substrates.* FEBS Lett, 1993. **322**(1): p. 51-5.

71. Agnes, R.S., et al., *Suborganelle sensing of mitochondrial cAMP-dependent protein kinase activity.* J Am Chem Soc, 2010. **132**(17): p. 6075-80.

72. Diviani, D., et al., *A-kinase anchoring proteins: scaffolding proteins in the heart.* Am J Physiol Heart Circ Physiol, 2011. **301**(5): p. H1742-53.

73. Welch, E.J., B.W. Jones, and J.D. Scott, *Networking with AKAPs: context-dependent regulation of anchored enzymes.* Mol Interv, 2010. **10**(2): p. 86-97.

74. Wong, W. and J.D. Scott, *AKAP signalling complexes: focal points in space and time.* Nat Rev Mol Cell Biol, 2004. **5**(12): p. 959-70.

75. Wang, L., et al., *Cloning and mitochondrial localization of full-length D-AKAP2, a protein kinase A anchoring protein.* Proc Natl Acad Sci U S A, 2001. **98**(6): p. 3220-5.

76. Grimsrud, P.A., et al., *A quantitative map of the liver mitochondrial phosphoproteome reveals posttranslational control of ketogenesis.* Cell Metab, 2012. **16**(5): p. 672-83.

77. Papa, S., et al., *cAMP-dependent protein kinase and phosphoproteins in mammalian mitochondria. An extension of the cAMP-mediated intracellular signal transduction.* FEBS Lett, 1999. **444**(2-3): p. 245-9.

78. Technikova-Dobrova, Z., et al., *Cyclic adenosine monophosphate-dependent phosphorylation of mammalian mitochondrial proteins: enzyme and substrate characterization and functional role.* Biochemistry, 2001. **40**(46): p. 13941-7.

79. Papa, S., *The NDUFS4 nuclear gene of complex I of mitochondria and the cAMP cascade.* Biochim Biophys Acta, 2002. **1555**(1-3): p. 147-53.

80. Piccoli, C., et al., *cAMP controls oxygen metabolism in mammalian cells.* FEBS Lett, 2006. **580**(18): p. 4539-43.

81. De Rasmo, D., et al., *Phosphorylation pattern of the NDUFS4 subunit of complex I of the mammalian respiratory chain.* Mitochondrion, 2010. **10**(5): p. 464-71.

82. Valenti, D., et al., *Deficit of complex I activity in human skin fibroblasts with chromosome 21 trisomy and overproduction of reactive oxygen species by mitochondria: involvement of the cAMP/PKA signalling pathway.* Biochem J, 2011. **435**(3): p. 679-88.

83. Raha, S., et al., *Control of oxygen free radical formation from mitochondrial complex I: roles for protein kinase A and pyruvate dehydrogenase kinase.* Free Radic Biol Med, 2002. **32**(5): p. 421-30.

84. Acin-Perez, R., et al., *Protein phosphorylation and prevention of cytochrome oxidase inhibition by ATP: coupled mechanisms of energy metabolism regulation.* Cell Metab, 2010. **13**(6): p. 712-9.

85. Acin-Perez, R., et al., *Modulation of mitochondrial protein phosphorylation by soluble adenylyl cyclase ameliorates cytochrome oxidase defects.* EMBO Mol Med, 2009. **1**(8-9): p. 392-406.

86. Lowell, B.B. and G.I. Shulman, *Mitochondrial Dysfunction and Type 2 Diabetes.* Science, 2005. **307**(5708): p. 384-387.

87. Huss, J.M. and D.P. Kelly, *Mitochondrial energy metabolism in heart failure: a question of balance.* J Clin Invest, 2005. **115**(3): p. 547-55.

88. Hafner, R.P. and M.D. Brand, *Hypothyroidism in rats does not lower mitochondrial ADP/O and H+/O ratios.* Biochem J, 1988. **250**(2): p. 477-84.

89. Fontaine, E.M., et al., *The yield of oxidative phosphorylation is controlled both by force and flux.* Biochem Biophys Res Commun, 1997. **232**(2): p. 532-5.

90. Kuznetsov, A.V., et al., *Striking Differences Between the Kinetics of Regulation of Respiration by ADP in Slow-Twitch and Fast-Twitch Muscles In Vivo.* European Journal of Biochemistry, 1996. **241**(3): p. 909-915.

91. Tonkonogi, M., et al., *Mitochondrial function and antioxidative defence in human muscle: effects of endurance training and oxidative stress.* J Physiol, 2000. **528 Pt 2**: p. 379-88.

92. Anderson, E.J. and P.D. Neufer, *Type II skeletal myofibers possess unique properties that potentiate mitochondrial H(2)O(2) generation.* Am J Physiol Cell Physiol, 2006. **290**(3): p. C844-51.

93. Perry, C.G., et al., *Inhibiting myosin-ATPase reveals a dynamic range of mitochondrial respiratory control in skeletal muscle.* Biochem J, 2011. **437**(2): p. 215-22.

94. Passarella, S., et al., *Increase in the ADP/ATP exchange in rat liver mitochondria irradiated in vitro by helium-neon laser.* Biochem Biophys Res Commun, 1988. **156**(2): p. 978-86.

95. Picard, M., et al., *Mitochondrial structure and function are disrupted by standard isolation methods.* PLoS One, 2011. **6**(3): p. e18317.

96. Roth, D.A. and G.A. Brooks, *Lactate and pyruvate transport is dominated by a pH gradient-sensitive carrier in rat skeletal muscle sarcolemmal vesicles.* Arch Biochem Biophys, 1990. **279**(2): p. 386-94.

97. Parker, N., et al., *Energization-dependent endogenous activation of proton conductance in skeletal muscle mitochondria.* Biochem J, 2008. **412**(1): p. 131-9.

98. Boudina, S., et al., *UCP3 Regulates Cardiac Efficiency and Mitochondrial Coupling in High Fat-Fed Mice but Not in Leptin-Deficient Mice.* Diabetes, 2012.

99. Echtay, K.S., et al., *Superoxide activates mitochondrial uncoupling proteins.* Nature, 2002. **415**(6867): p. 96-9.

100. De Sousa, E., et al., *Subcellular creatine kinase alterations. Implications in heart failure.* Circ Res, 1999. **85**(1): p. 68-76.

101. De Sousa, E., et al., *Heart failure affects mitochondrial but not myofibrillar intrinsic properties of skeletal muscle.* Circulation, 2000. **102**(15): p. 1847-53.

102. Lienhard, G.E. and Secemski, II, *P 1 ,P 5 -Di(adenosine-5')pentaphosphate, a potent multisubstrate inhibitor of adenylate kinase.* J Biol Chem, 1973. **248**(3): p. 1121-3.

103. Kemp, G.J., et al., *Interrelations of ATP synthesis and proton handling in ischaemically exercising human forearm muscle studied by 31P magnetic resonance spectroscopy.* J Physiol, 2001. **535**(Pt 3): p. 901-28.

104. Roth, K. and M.W. Weiner, *Determination of cytosolic ADP and AMP concentrations and the free energy of ATP hydrolysis in human muscle and brain tissues with 31P NMR spectroscopy.* Magn Reson Med, 1991. **22**(2): p. 505-11.

105. Katz, L.A., et al., *Relation between phosphate metabolites and oxygen consumption of heart in vivo.* Am J Physiol, 1989. **256**(1 Pt 2): p. H265-74.

106. Di Benedetto, G., et al., *Ca2+ and cAMP cross-talk in mitochondria.* J Physiol, 2014. **592**(Pt 2): p. 305-12.

107. Valsecchi, F., et al., *cAMP and mitochondria.* Physiology (Bethesda), 2013. **28**(3): p. 199-209.

108. Pagliarini, D.J., et al., *A mitochondrial protein compendium elucidates complex I disease biology.* Cell, 2008. **134**(1): p. 112-23.

109. Papa, S., et al., *Respiratory chain complex I, a main regulatory target of the cAMP/PKA pathway is defective in different human diseases.* FEBS Lett, 2012. **586**(5): p. 568-77.

110. Zippin, J.H., et al., *Compartmentalization of bicarbonate-sensitive adenylyl cyclase in distinct signaling microdomains.* FASEB J, 2003. **17**(1): p. 82-4.

111. Tonkonogi, M., et al., *Reduced oxidative power but unchanged antioxidative capacity in skeletal muscle from aged humans.* Pflugers Arch, 2003. **446**(2): p. 261-9.

112. Gilliam, L.A., et al., *The anticancer agent doxorubicin disrupts mitochondrial energy metabolism and redox balance in skeletal muscle.* Free Radic Biol Med, 2013. **65**: p. 988-96.

113. Anderson, E.J., et al., *Do Fish Oil Omega-3 Fatty Acids Enhance Antioxidant Capacity and Mitochondrial Fatty Acid Oxidation in Human Atrial Myocardium via PPARgamma Activation?* Antioxid Redox Signal, 2014. **2014**: p. 10.

114. Lambert, A.J. and M.D. Brand, *Inhibitors of the quinone-binding site allow rapid superoxide production from mitochondrial NADH:ubiquinone oxidoreductase (complex I).* J Biol Chem, 2004. **279**(38): p. 39414-20.

115. Hess, K.C., et al., *The "soluble" adenylyl cyclase in sperm mediates multiple signaling events required for fertilization.* Dev Cell, 2005. **9**(2): p. 249-59.

116. Maren, T.H., *A simplified micromethod for the determination of carbonic anhydrase and its inhibitors.* J Pharmacol Exp Ther, 1960. **130**: p. 26-9.

117. Mitchell, P. and J. Moyle, *Acid-base titration across the membrane system of rat-liver mitochondria. Catalysis by uncouplers.* Biochem J, 1967. **104**(2): p. 588-600.

118. Tian, G., et al., *Glucose- and hormone-induced cAMP oscillations in alpha- and beta-cells within intact pancreatic islets.* Diabetes, 2011. **60**(5): p. 1535-43.

119. Bitterman, J.L., et al., *Pharmacological distinction between soluble and transmembrane adenylyl cyclases.* J Pharmacol Exp Ther, 2013. **347**(3): p. 589-98.

120. Steegborn, C., et al., *A novel mechanism for adenylyl cyclase inhibition from the crystal structure of its complex with catechol estrogen.* J Biol Chem, 2005. **280**(36): p. 31754-9.

121. Fussell, K.C., et al., *Catechol metabolites of endogenous estrogens induce redox cycling and generate reactive oxygen species in breast epithelial cells.* Carcinogenesis, 2011. **32**(8): p. 1285-93.

122. Chijiwa, T., et al., *Inhibition of forskolin-induced neurite outgrowth and protein phosphorylation by a newly synthesized selective inhibitor of cyclic AMP-dependent protein kinase, N-[2-(p-bromocinnamylamino)ethyl]-5-isoquinolinesulfonamide (H-89), of PC12D pheochromocytoma cells.* J Biol Chem, 1990. **265**(9): p. 5267-72.

123. Livigni, A., et al., *Mitochondrial AKAP121 links cAMP and src signaling to oxidative metabolism.* Mol Biol Cell, 2006. **17**(1): p. 263-71.

124. Zhao, X., et al., *Phosphoproteome analysis of functional mitochondria isolated from resting human muscle reveals extensive phosphorylation of inner membrane protein complexes and enzymes.* Mol Cell Proteomics, 2011. **10**(1): p. M110 000299.

125. Mitchell, P. and J. Moyle, *Chemiosmotic hypothesis of oxidative phosphorylation.* Nature, 1967. **213**(5072): p. 137-9.

126. Kakiuchi, S. and R. Yamazaki, *Calcium dependent phosphodiesterase activity and its activating factor (PAF) from brain studies on cyclic 3',5'-nucleotide phosphodiesterase (3).* Biochem Biophys Res Commun, 1970. **41**(5): p. 1104-10.

127. Kleinboelting, S., et al., *Crystal structures of human soluble adenylyl cyclase reveal mechanisms of catalysis and of its activation through bicarbonate.* Proc Natl Acad Sci U S A, 2014. **111**(10): p. 3727-32.

128. Davies, S.P., et al., *Specificity and mechanism of action of some commonly used protein kinase inhibitors.* Biochem J, 2000. **351**(Pt 1): p. 95-105.

129. Gnaiger, E., *Oxygen conformance of cellular respiration. A perspective of mitochondrial physiology.* Adv Exp Med Biol, 2003. **543**: p. 39-55.

130. Varikmaa, M., et al., *Role of mitochondria-cytoskeleton interactions in respiration regulation and mitochondrial organization in striated muscles.* Biochim Biophys Acta, 2014. **1837**(2): p. 232-45.

131. Kay, L., et al., *Study of regulation of mitochondrial respiration in vivo. An analysis of influence of ADP diffusion and possible role of cytoskeleton.* Biochim Biophys Acta, 1997. **1322**(1): p. 41-59.

132. Saks, V.A., et al., *Permeabilized cell and skinned fiber techniques in studies of mitochondrial function in vivo.* Mol Cell Biochem, 1998. **184**(1-2): p. 81-100.

133. Veksler, V.I., et al., *Muscle creatine kinase-deficient mice. II. Cardiac and skeletal muscles exhibit tissue-specific adaptation of the mitochondrial function.* J Biol Chem, 1995. **270**(34): p. 19921-9.

134. Hogan, M.C., et al., *Maximal O2 uptake of in situ dog muscle during acute hypoxemia with constant perfusion.* J Appl Physiol (1985), 1990. **69**(2): p. 570-6.

135. Hogan, M.C., et al., *Limitation of maximal O2 uptake and performance by acute hypoxia in dog muscle in situ.* J Appl Physiol (1985), 1988. **65**(2): p. 815-21.

136. Vaupel, P., F. Kallinowski, and P. Okunieff, *Blood flow, oxygen and nutrient supply, and metabolic microenvironment of human tumors: a review.* Cancer Res, 1989. **49**(23): p. 6449-65.

137. Majewski, N., et al., *Hexokinase-mitochondria interaction mediated by Akt is required to inhibit apoptosis in the presence or absence of Bax and Bak.* Mol Cell, 2004. **16**(5): p. 819-30.

138. Sun, L., et al., *Glucose phosphorylation and mitochondrial binding are required for the protective effects of hexokinases I and II.* Mol Cell Biol, 2008. **28**(3): p. 1007-17.

139. Han, Y.H., et al., *Effects of carbonyl cyanide p-(trifluoromethoxy) phenylhydrazone on the growth inhibition in human pulmonary adenocarcinoma Calu-6 cells.* Toxicology, 2009. **265**(3): p. 101-7.

140. Lou, P.H., et al., *Mitochondrial uncouplers with an extraordinary dynamic range.* Biochem J, 2007. **407**(1): p. 129-40.

141. Pan, X., et al., *The physiological role of mitochondrial calcium revealed by mice lacking the mitochondrial calcium uniporter.* Nat Cell Biol, 2013. **15**(12): p. 1464-72.

142. Rizzuto, R., et al., *Microdomains with high Ca2+ close to IP3-sensitive channels that are sensed by neighboring mitochondria.* Science, 1993. **262**(5134): p. 744-7.

143. Carafoli, E., et al., *The release of calcium from heart mitochondria by sodium.* J Mol Cell Cardiol, 1974. **6**(4): p. 361-71.

144. Palty, R., et al., *NCLX is an essential component of mitochondrial Na+/Ca2+ exchange.* Proc Natl Acad Sci U S A, 2010. **107**(1): p. 436-41.

145. Bergen, W.G. and R.A. Merkel, *Body composition of animals treated with partitioning agents: implications for human health.* Faseb j, 1991. **5**(14): p. 2951-7.

146. Hoshino, D., et al., *Clenbuterol, a beta2-adrenergic agonist, reciprocally alters PGC-1 alpha and RIP140 and reduces fatty acid and pyruvate oxidation in rat skeletal muscle.* Am J Physiol Regul Integr Comp Physiol, 2012. **302**(3): p. R373-84.

147. Mounier, R., et al., *Molecular impact of clenbuterol and isometric strength training on rat EDL muscles.* Pflugers Arch, 2007. **453**(4): p. 497-507.

148. Torgan, C.E., et al., *Fiber type-specific effects of clenbuterol and exercise training on insulin-resistant muscle.* J Appl Physiol (1985), 1995. **79**(1): p. 163-7.

149. Sundal, S. and S. Sharma, *Ultrastructural findings for the mitochondrial subpopulation of mice skeletal muscle after adrenergic stimulation by clenbuterol.* J Physiol Sci, 2007. **57**(1): p. 7-14.

150. Baradaran, R., et al., *Crystal structure of the entire respiratory complex I.* Nature, 2013. **494**(7438): p. 443-8.

151. Amano, M., M. Nakayama, and K. Kaibuchi, *Rho-kinase/ROCK: A key regulator of the cytoskeleton and cell polarity.* Cytoskeleton (Hoboken), 2010. **67**(9): p. 545-54.

152. Del Re, D.P., S. Miyamoto, and J.H. Brown, *RhoA/Rho kinase up-regulate Bax to activate a mitochondrial death pathway and induce cardiomyocyte apoptosis.* J Biol Chem, 2007. **282**(11): p. 8069-78.

153. Deluca, H.F. and G.W. Engstrom, *Calcium uptake by rat kidney mitochondria.* Proc Natl Acad Sci U S A, 1961. **47**: p. 1744-50.

154. Han, X.J., et al., *CaM kinase I alpha-induced phosphorylation of Drp1 regulates mitochondrial morphology.* J Cell Biol, 2008. **182**(3): p. 573-85.

East Carolina University

1907-2007 CENTENNIAL

Animal Care and Use Committee
212 Ed Warren Life Sciences Building
East Carolina University
Greenville, NC 27834

252-744-2436 office
252-744-2355 fax

December 4, 2009

Darrell Neufer, Ph.D.
Department of Physiology
Brody 6N-98
ECU Brody School of Medicine

Dear Dr. Neufer:

Your Animal Use Protocol entitled, "Breeding of Mice for Mitochondrial Bioenergetics and Metabolic Disease Studies," (AUP #Q285) was reviewed by this institution's Animal Care and Use Committee on 12/3/09. The following action was taken by the Committee:

"Approved as submitted"

Note: Please send a registration to the Biological Safety Committee for the breeding of transgenic/outcross animals.

A copy is enclosed for your laboratory files. Please be reminded that all animal procedures must be conducted as described in the approved Animal Use Protocol. Modifications of these procedures cannot be performed without prior approval of the ACUC. The Animal Welfare Act and Public Health Service Guidelines require the ACUC to suspend activities not in accordance with approved procedures and report such activities to the responsible University Official (Vice Chancellor for Health Sciences or Vice Chancellor for Academic Affairs) and appropriate federal Agencies.

Sincerely yours,

Robert G. Carroll, Ph.D.
Chairman, Animal Care and Use Committee

RGC/jd

enclosure